1971

Capillary-reservoir diffusion studies in Hg-In alloys utilizing continuous resistivity measurement of composition

Robert Hamilton Kaiser
Iowa State University

Capillary-reservoir diffusion studies in Hg-In alloys utilizing continuous resistivity measurement of composition

by

Robert Hamilton Kaiser

A Dissertation Submitted to the
Graduate Faculty in Partial Fulfillment of
The Requirements for the Degree of
DOCTOR OF PHILOSOPHY

Major Subject: Chemical Engineering

Approved:

Signature was redacted for privacy.

In Charge of Major Work

Signature was redacted for privacy.

For the Major Department

Signature was redacted for privacy.

For the Graduate College

Iowa State University
Ames, Iowa

1971

TABLE OF CONTENTS

INTRODUCTION

Suggestions for improvement of metallurgical production and purification through such processes as distillation, zone refining, and slag-metal contacting have drawn attention to the determination of liquid metal diffusion coefficients for applied purposes. In addition, a fundamental study of the liquid state requires a better understanding of the diffusion process.

Several techniques have been utilized for liquid metal diffusion studies, but the capillary-reservoir system has received the widest acceptance due to its simplicity. Regardless of which method or which calculation procedure is used, the determination of a measured composition ratio is inevitable. Yet composition is the single most difficult parameter to measure accurately.

The goal of this study was to design a capillary-reservoir apparatus which would continuously measure the average composition of the material in the capillary without affecting the diffusion process. The property of electrical resistivity was employed to determine composition. It was anticipated that this would provide for ease and precision in gathering data while eliminating the handling steps prevalent in most other techniques. For simplicity, the mercury-indium system was examined at room temperature.

PREVIOUS WORK

The problems inherent in the measurement of liquid metal properties have led to a variety of schemes and devices for the determination of their diffusion coefficients. The ingenuity of investigators attempting to overcome major difficulties in diffusion measurements has frequently resulted in either a failure to solve the problem intended or the creation of a new one. Quoting the German chemist Wilhelm Ostwald, W. C. Roberts-Austen (34) wrote, ". . . to make accurate experiments in diffusion is one of the most difficult problems in practical physics." Generally, for liquid metals these problems include 1) the handling of samples at molten metal temperatures, 2) the creation of convective motion of the system being investigated, and 3) the accurate determination of the composition changes that occur during the diffusion process.

Some examples of various methods of studying liquid metal diffusion can be categorized as follows:

Method	References
1) Electrotransport Cell	(27), (45)
2) EMF Techniques	(8), (13), (40)
3) Shear Cell	(2), (30)
4) Diaphragm Cell	(4), (7), (31)
5) Capillary Techniques	

Only the capillary techniques, which have received the widest

attention, will be surveyed here.

In the late nineteenth century W. C. Roberts-Austen (34) performed experiments on several binary liquid metal systems using the method which has come to be called the capillary-reservoir technique. This procedure involves the submersion of a small tube sealed at one end filled with a known alloy composition into a reservoir of a second alloy. Diffusion is then permitted to progress for a given length of time following which the tube is withdrawn from the bath. The change in composition of the material in the tube is noted, and the diffusion coefficient is determined from the proper solution of Fick's Second Law for one-dimensional diffusion assuming constant diffusivity,

$$\frac{\partial C}{\partial t} = D\frac{\partial^2 C}{\partial x^2} . \qquad (1)$$

In his initial work Roberts-Austen allowed a capillary filled with pure lead to diffuse upward into a gold-lead alloy. At the conclusion of a run the capillary tube material was allowed to solidify and was then cut into sections each of which was analyzed for composition. The solution of Fick's Law was accomplished with the aid of the Stefan-Kawalki Tables (21). When one considers the crude measuring and control devices that Roberts-Austen must have employed over 70 years ago, it is interesting to observe his rather reasonable results. Comparing, for example, his data on silver and tin

taken in 1896 with that reported by Davis and Fryzuk (11) in 1965, Roberts-Austen obtained a value of 4.8×10^{-5} cm^2/sec while the more recent investigation yielded a slightly higher value of 5.6×10^{-5} cm^2/sec. Although Roberts-Austen may have made serious errors such as employing an inverted density gradient as was the case in the Pb-Au system, his version of the capillary-reservoir technique and its mechanics has not changed appreciably to this day.

In 1949, Anderson and Saddington (1) applied a radioactive tracer concentration determination to the capillary-reservoir system in their study of self-diffusion in poly-tungstate acids. The importance of this development lies in the fact that if the self-diffusion coefficients can be determined for a material, then the mutual diffusion coefficients of two diffusing species with similar ionic radii can be estimated. (The last statement assumes that the ionic radius is known.) This technique was first applied to liquid metals in 1952 by Hoffman (20) while measuring the self-diffusion coefficient of mercury.

Applying tracer determinations, Careri et al. (6) reported a different capillary technique in 1954 for the measurement of diffusion in liquid metals. Studying the self-diffusion of indium, a long porcelain capillary tube was filled half with solid labelled indium and half with nonactivated solid indium. When melted, this amounted to contacting two semi-

infinite rods of liquid metal. After melting, the capillary contents were brought "rapidly to a controlled temperature" and allowed to diffuse for a given length of time. Following solidification, the diffusion coefficient was computed by determining the activity at different points in the rod. Although some question may be raised as to the initial time and temperature at which diffusion commenced, this study demonstrated the feasibility of the long capillary method coupled with the tracer technique for liquid metals.

Grace and Derge (17) measured the diffusion coefficient of bismuth in lead in 1955 with a capillary-reservoir technique. In order to insure a well-mixed bath, nitrogen was bubbled into the melt. Since the lead-bismuth alloy in the capillary was allowed to diffuse upward into a bath of pure lead (sp. g. 11.3), a serious inverted composition gradient was established for large bismuth (sp. g. 9.8) compositions of the alloy. This fact may account for the apparent diffusion coefficients one and two orders of magnitude higher than expected. This dilemma has been studied by Powers (33) and Stahlhut (38).

In 1957 Niwa et al. (32) presented the results of diffusion studies on several molten metal systems performed by three different experimental methods. The first of these involved a capillary-reservoir system similar to those previously mentioned using a capillary 3 mm in diameter by 5 cm long. The second method is similar to that used by

Careri et al. (6) employing two semi-infinite rods of different alloy compositions. Their final technique involved the contacting of a semi-infinite rod of pure component material with a finite cylinder of a differing alloy composition. In each of these cases diffusion was allowed to proceed for a certain length of time following which the components were solidified, sectioned, and analyzed. These methods are each characterized by the preparation of a sample, solidification, remelting for the diffusion run, and finally resolidification before analysis. This process would tend to suggest the possibility of some alloy segregation. Also, in the case of the second and third techniques, there appears to be some question as to what initial condition exists at the dissimilar alloy interface.

Investigating the diffusion of various solutes in liquid tin, Ma and Swalin (23) developed in 1959 a capillary-reservoir device which was to be used by several subsequent experimenters. A capillary of alloy material (prepared external to the diffusion device) was lowered into a pure tin melt over which an inert atmosphere was maintained. Following diffusion, the capillary material was solidified and analyzed chemically with the aid of a spectrophotometer. Several years later Ma and Swalin (24) utilized this equipment to study self-diffusion in liquid tin with the radioactive technique of Anderson and Saddington (1). Applying

tracers to this method for solute diffusion were Davis and Fryzuk (11) and Gupta and Wang (18). In all of these investigations the capillary was located vertically in the reservoir. Since there was a growing concern at this stage of development for the effect of convection in capillary measurements, Leak and Swalin (22) felt it essential to orient the capillary in a horizontal plane ". . . to minimize the effects of convection currents." However, it has since been shown by Verhoeven (43) that this horizontal positioning actually increases the convective effect.

In the mid 1960's, Hesson and Burris (19) and Mirshamsi et al. (29) altered the Ma and Swalin device by slowly rotating the capillary in the reservoir in order to sweep away any buildup of diffusate in the region near the capillary mouth.

Recent work at the Ames Laboratory has attempted to modify these capillary diffusion techniques. An apparatus first reported by Powers (33) while examining diffusion and convection in the mercury-indium system showed how the capillary and reservoir material could be prepared simultaneously and independently in the diffusion cell thereby overcoming the melting-solidification cycle that would occur with higher melting alloys. This operation would tend to eliminate much of the convection produced by capillary immersion and subsequent withdrawal. After diffusion the capillary could be

isolated from the reservoir and the contents analyzed chemically with a spectrophotometer. Since the entire capillary was analyzed for its average composition, an alloy segregation occurring following the conclusion of a run was unimportant. This technique has been modified successfully by Wenger (46) in his determination of diffusion coefficients in indium-tin alloys at 300 ^{o}C.

Regardless of the diffusion device being used in most studies, only the initial and final compositions are determined, and therefore, a knowledge of the composition-time profile is unknown. A few investigators have attempted to monitor the diffusion process on a continuous basis. Studying resistivity, electric mobility, and diffusion in cadmium amalgams, Mangelsdorf (27) has reported a ribbon-shaped capillary cell. Foils made of 0.001 inch iron were placed at several locations along a capillary which was in contact with a reservoir. By noting the history of electric potential differences between the electrodes, the diffusion process could be followed. Buell and Shuck (3) have also designed a resistivity measuring scheme to monitor diffusion. A ten centimeter glass capillary with reservoirs on either end was filled one half with pure bismuth and one half with pure tin. Tungsten electrodes were sealed in the tube at intervals along its length. By permitting diffusion to take place for about ten days a quasi-steady state could be attained. Concen-

tration (resistivity) data were taken for a period of time to determine a relative diffusion coefficient. Both the capillary and the reservoirs of this device could be filled with metal in a single operation while also monitoring the diffusion process, thus eliminating the melting-solidification cycle. Recently, Castleman (7) applied a radioactive tracer technique to a diaphragm cell study of mercury self-diffusion. The counter was positioned so that the radioactivity of the mercury tracer in the lower reservoir could be noted continuously. These continuous measurements all enjoy the advantage of providing information as to the history of the diffusion process while eliminating the handling step required to determine a final composition.

In an attempt to better understand the liquid state, many theories have been proposed to describe liquid diffusion. The Stokes-Einstein (15), Sutherland-Einstein (41), and Eyring (16) equations relate the diffusion coefficient to the viscosity, temperature, and the size of the diffusing species. Though similar in form, these three equations vary from each other by a constant of substantial magnitude. Thus, when an experimenter compares his diffusion data to one of these models, good agreement with any one of them precludes agreement with the others. The Sutherland-Einstein equation fits some liquid metal data well if the size parameter is taken as the Pauling univalent radius (44). Swalin (42) and

Walls and Upthegrove (44) have developed rather complex equations relating the diffusion coefficient to such parameters as the latent heat of vaporization and an activation entropy. Practically, these relations become cumbersome due to the difficulty of evaluating the numerous parameters.

Much of the experimental data on liquid metal diffusion has been correlated as an Arrhenius equation:

$$D = D_o \exp(-Q_o/RT) \qquad (2)$$

where

D_o = frequency factor

Q_o = activation energy.

Swalin (42) states that the only basis for utilizing such an equation is that it seems to fit the data over small temperature ranges.

The treatments thus far described attempt to relate the diffusion coefficient to a function of temperature. Darken (10) has shown that the composition dependence of the mutual diffusion coefficient can be expressed as:

$$D = (N_1 D_2^* + N_2 D_1^*)\left(1 + N_1 \frac{\partial \ln \nu_1}{\partial N_1}\right) \qquad (3)$$

where

D_i^* = diffusivity of i determined by a tracer technique in an alloy of the same composition

ν_i = activity coefficient of i.

Since a suitable model has not yet been developed that will describe all liquids (44), it is difficult to model the transport properties in all liquids with a single expression. These models may, however, serve as a basis of comparison with the experimental data.

THEORY

Diffusion Coefficient Calculation

Although the capillary-reservoir technique itself is somewhat standard, the computation of a diffusion coefficient can be made in a number of different ways. All of these calculations begin with a solution of Fick's Second Law which states:

$$\frac{\partial C}{\partial t} = D\frac{\partial^2 C}{\partial x^2} . \qquad (4)$$

This equation assumes 1) unidirectional diffusion, 2) absence of bulk flow, 3) constant temperature, 4) constant density, and 5) a constant diffusion coefficient. The first of these assumptions is validated due to the geometry of a capillary-reservoir system as long as no inverted density gradients are used. Constant temperature can be attained through careful experimentation. The constancy of the physical properties ρ and D are approximated if small composition gradients are employed. The "C's" used in Equation 4 refer to any appropriate molar composition units. Atomic fractions will subsequently be utilized as in Equation 5,

$$\frac{\partial N}{\partial t} = D\frac{\partial^2 N}{\partial x^2} . \qquad (5)$$

The selection of the boundary conditions at this point determines the final form of the diffusion coefficient computation.

If the capillary is considered to be very long or the diffusion time short such that the dimensionless group $Dt/L^2 < 0.1$, the boundary conditions become

$$\begin{array}{lllll} \text{I.C.} & t = 0 & N = N_o & , & x > 0 \\ \text{B.C. 1} & x = 0 & N = N_R & , & t \geq 0 \\ \text{B.C. 2} & x \to \infty & N = N_o & , & t \geq 0 \end{array} \quad . \tag{6}$$

Equation 5 is then solved by a combination of variables technique to obtain

$$\theta(x,t) = \frac{N-N_R}{N_o-N_R} = 1 - \text{erf}\left(\frac{x}{2\sqrt{Dt}}\right) . \tag{7}$$

Analysis of the capillary contents at various points along its length is required for application of Equation 7. This method has been used by Davis and Fryzuk (11) and Niwa et al. (32). The Stefan-Kawalki Table used by Roberts-Austen (34) is an application of Equation 7. The average composition can be determined with the aid of an overall mass balance on the capillary (17) to give

$$\bar{\theta}(t) = \frac{\bar{N}-N_R}{N_o-N_R} = 1 - \left(\frac{2}{L}\right)\left(\frac{Dt}{\pi}\right)^{1/2} . \tag{8}$$

Used by Gupta and Wang (18) and Grace and Derge (17), this solution lends itself to a single average composition measurement and skirts the problem of alloy segregation within the capillary on solidification.

Another solution for Equation 5 is obtained if the second boundary condition in Equations 6 is changed to the

flux condition

$$\text{B.C. 2} \qquad x = L \qquad \frac{\partial N}{\partial x} = 0 \ , \quad t \geq 0 \ . \tag{9}$$

For this case the method of separation of variables is employed to yield the series solution

$$\Theta(x,t) = \frac{N-N_R}{N_o-N_R} = \frac{4}{\pi} \sum_{n=0}^{\infty} \left(\frac{1}{2n+1}\right) \exp\left[\frac{-\pi^2}{4}(2n+1)^2 \frac{Dt}{L^2}\right] \left[\sin \frac{\pi}{2L}(2n+1)x\right] . \tag{10}$$

Typically, it is desired to know the average composition over the total length of the capillary, so Equation 10 is integrated from x = 0 to x = L yielding

$$\overline{\Theta}(t) = \frac{\overline{N}-N_R}{N_o-N_R} = \frac{8}{\pi^2} \sum_{n=0}^{\infty} \left(\frac{1}{2n+1}\right)^2 \exp\left[\frac{-\pi^2}{4}(2n+1)^2 \frac{Dt}{L^2}\right]. \tag{11}$$

Equation 11 converges rapidly if the dimensionless group $Dt/L^2 > 0.25$ (12) and can be truncated after the first term to give

$$\overline{\Theta}(t) = \frac{\overline{N}-N_R}{N_o-N_R} = \frac{8}{\pi^2} \exp\left[\frac{-\pi^2 Dt}{4L^2}\right]. \tag{12}$$

This truncation is based on the fact that the errors in composition determination are much greater in magnitude than those created by series truncation. Equation 12 is useful for shorter capillaries when a single endpoint composition measurement is made. It is required, however, that the minimum diffusion time be on the order of one or two days

for typical capillaries.

Ultimately in this work it was necessary to know the average composition between any two points in the capillary. Equation 10 can be integrated along the capillary length from αL to βL to give

$$\bar{\theta}(t) = \frac{\bar{N}-N_R}{N_o-N_R} = \frac{8}{\pi^2} \sum_{n=0}^{\infty} \frac{1}{(2n+1)^2(\beta-\alpha)} \exp\left[\frac{-\pi^2}{4}(2n+1)^2 \frac{Dt}{L^2}\right] \left[\cos\frac{\alpha\pi}{2}(2n+1) - \cos\frac{\beta\pi}{2}(2n+1)\right] \tag{13}$$

where

α, β = fractions of total capillary lengths such that $0 \leq \alpha < \beta \leq 1$.

The details of this integration are shown in Appendix A.

Resistivity Measurements

For a cylindrical column of material the electrical resistivity is defined as

$$\rho_e = R\left(\frac{A}{L}\right) \tag{14}$$

where

R = electrical resistance along the length of the column

A = cross sectional area of the column

L = length of the column.

Thus, for a capillary of given geometry the electrical resistivity is proportional to the resistance. If a constant

direct current is applied, Ohm's Law states that the voltage is proportional to resistance and hence to resistivity. Further, since the resistivity of a material, say a binary liquid metal alloy, is a function of its composition at a constant temperature, changes in voltage drop across the material can be related to composition changes. As is the case with the metals used in this study, mercury and indium, a resistivity measurement of composition would best be accomplished if the pure component resistivities of the binary were considerably different. In addition, the mercury-indium system lends itself to this type of measurement since the greatest changes in resistivity with composition occur for small amounts of indium in the amalgam (9).

Resistivity measurements are made by passing a known direct current through a material of known geometry. At locations in the material inside the points at which the current leads are attached, voltage taps are installed. This "four-probe" measurement (two current and two potential leads) insures that only the resistance of the unknown material is being measured. If the current and potential leads were in common, the voltage observed would be due to the unknown material plus the potential drop in the leads plus that due to the contact resistances. The resistances of the leads becomes significant in precision resistance measurements of less than 0.1 ohm (28). At first it was hoped to accomplish the resistivity measurements in the

capillary-reservoir diffusion system using only two probes with the hope that the extra lead and contact resistance could be accounted for in the geometric calibration, (A/L). This, however, proved to be impossible, and a true "four-probe" measurement was eventually devised.

By measuring composition changes by resistivity changes in a liquid metal two deleterious side effects can occur. First, the passage of direct current may tend to separate the binary components by electrotransport creating a flux in addition to the molecular flux being observed. By reversing the direction of the current at equal intervals this extra flux can be cancelled. Second, thermocouple voltages can arise through the several changes of conducting material in the potential measuring circuit. This phenomenon, termed the Seebeck effect (14), can be negated if all of these junctions are at a constant temperature.

EXPERIMENTAL

Equipment Design

Diffusion cell

The diffusion cell used in this work evolved through three stages of development. Figure 1 is an exploded pictorial of Cell III, the final design.

The basic diffusion cell, similar to that reported by Powers (33), was constructed from Plexiglas and Kel-F, a fluorocarbon made by 3-M Company. The design permitted six simultaneous, independent diffusion measurements. The capillary section has been revised from that of Powers in order to accommodate the necessary electrodes. Kel-F, used for the three inch diameter channel and reservoir sections, permitted the Kel-F-Plexiglas surfaces to be held together tight enough for a liquid metal seal without severely scoring each other when rotated. The reservoirs were one-half inch in diameter and located 60° apart. The channel section allowed for the filling of the capillaries with liquid metal from bottom to top. The capillary, reservoir, and channel sections were aligned on a threaded nylon rod, and intimate contact was maintained by tightening the sections together with nylon nuts.

The variations in cell design referred to previously involved modifications of the capillary section to accommodate

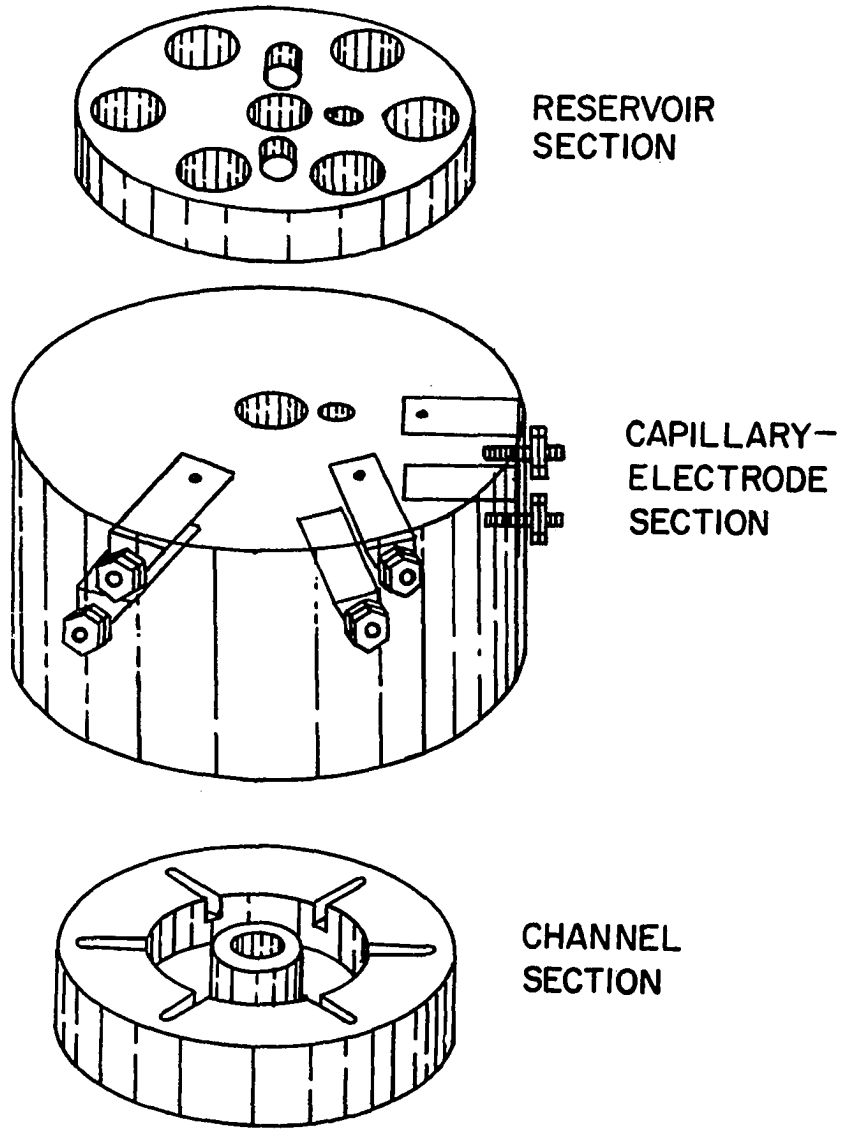

Figure 1. Exploded pictorial of Cell III

potential and current carrying electrodes. Cell I was identical to the Powers cell except that thin strips of stainless steel sheet were recessed into both sides of the capillary section at each capillary location. Six 0.04 inch capillary holes and a 1/4 inch filling hole were bored through the two inch thick Plexiglas. Stainless steel wires were then welded to these strips, and thus current could be carried to the capillary. By attaching voltage measuring leads to this same stainless wire it was hoped that the resistivity of the liquid metal in the capillary could be monitored continuously. This proved unsatisfactory since the magnitude of the contact and lead resistances was so great that precision in the resistivity determination was severely impaired. Also, when pure mercury was placed in the capillary at constant temperature with this "two-probe" scheme, the observed resistance tended to increase significantly with time. Therefore, the idea of including the added resistance of the contacts and leads with the geometric calibration factor, (A/L), had to be abandoned.

In order to escape this dilemma it was necessary to separate the current and potential electrodes completely by devising a "four-probe" technique as suggested by Meaden (28). The new capillary design, Cell II, was identical to Powers' but without the channel section. A Cell II schematic with the electrodes made of cladded heating wire is shown

in Figure 2. Made by American Standard under the trade name Aerocoax, these probes consist of a 26 gauge nichrome wire oriented coaxially inside an inconel sheath with a 0.040 inch outside diameter. The nichrome is insulated from the inconel with a tightly packed magnesium oxide powder. Using this type of conductor the potential leads could be attached to the nichrome and the current leads to the inconel thereby separating the potential and current circuits and creating a modified "four-probe" technique. At the end where the electrode was to contact the liquid metal, the electrode was ground flat on a polishing wheel. At the opposite end the attachment was made to the potential and current circuits. As shown in Figure 2, current leads were soft soldered directly to the inconel sheath. This sheath was stripped exposing the nichrome to which a copper tube connector was crimped as nichrome may not easily be soldered. At the point where the nichrome extended beyond the inconel sheath, a drop of epoxy glue insured no shorting between the conductors. Figure 2 shows the placement of the electrodes in the capillary and reservoir. Since the capillary and the sheath were both 0.040 inch in diameter, a snug fit was possible for the capillary electrodes. To insure that the penetration into the capillary was constant, a Plexiglas collar was fitted around the electrode permitting it to extend about 1/16 inch into the capillary. The reservoir

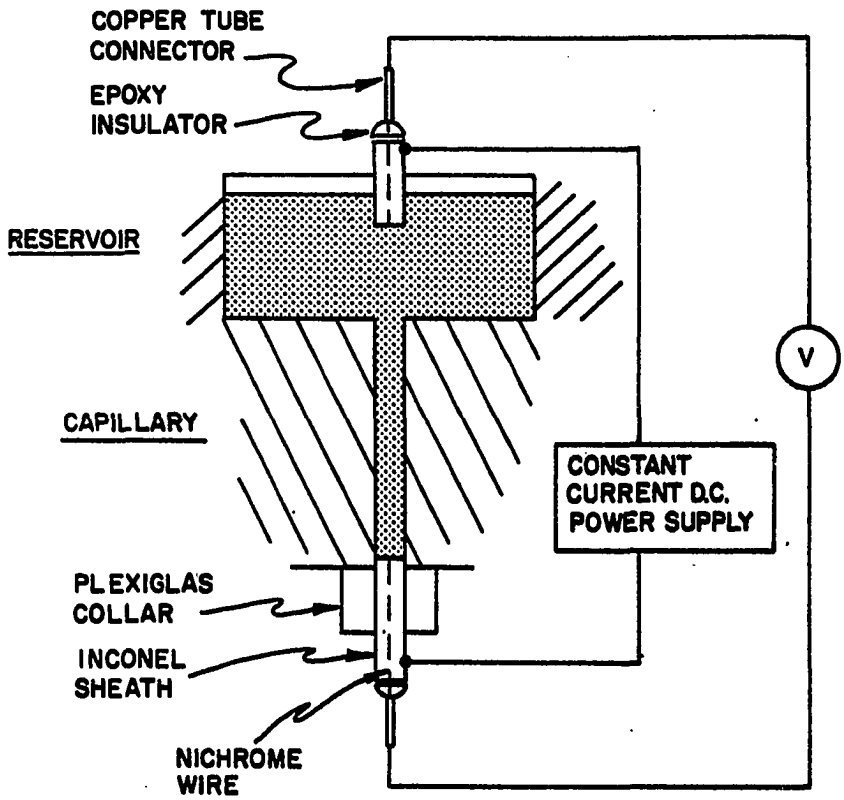

Figure 2. Schematic drawing of Cell II measurement

electrode was suspended in the bath to a depth of about 1/8 inch. Since the resistance is inversely proportional to the geometric constant (A/L),

$$R_{Res} = R_{Cap}\left[\frac{(\frac{A}{L})_{Cap}}{(\frac{A}{L})_{Res}}\right] = \left[\frac{(\frac{0.00119}{2.0})}{(\frac{0.196}{0.5})}\right]R_{Cap} = 0.00152\ R_{Cap}\ . \tag{15}$$

This fact shows that the resistance across the reservoir is negligible when compared to that across the capillary. Therefore, the observed resistance between the probes is very nearly the resistance across the capillary.

After data were taken with Cell II, a considerable amount of capillary erosion was observed to have taken place as a result of the removable lower electrode. At most, five or six runs could be made before the capillary-electrode fit became sloppy causing a leakage of liquid metal. Since it was necessary to determine the working geometric constant, (A/L), of each capillary, at least two runs were required just for calibration. This left a three or four run diffusion-life span for each cell. It was decided that the electrodes had to become a permanent part of the cell.

Figure 3 shows a schematic, and Figure 1 shows an exploded pictorial of Cell III with its stationary electrodes. The capillary electrodes, made from 0.003 inch strips of molybdenum sheet, were laminated between layers of Plexiglas using liquid Plexiglas cement. The molybdenum that extended

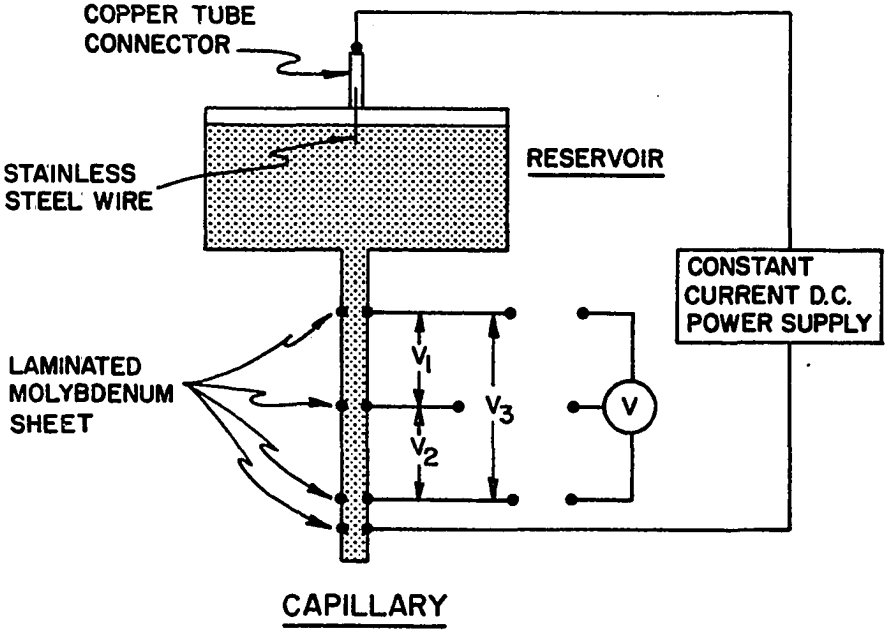

Figure 3. Schematic drawing of Cell III measurement

beyond the radius of the capillary section was folded along the side of the section and secured with a stainless steel stud and nut. In this way the electrical connection could be made directly to the stud. The six capillary holes were then drilled through the two inch Plexiglas-molybdenum composite. The electrode, then, was in the form of an annulus within the capillary and did not itself interfere with the cross section. Cell III was then assembled and filled like Cell I. In order to make resistivity measurements, a stainless steel electrode was suspended in the reservoir and current was passed from this electrode to the lowest molybdenum electrode in the laminate. Voltage drops then were measured between any two of the remaining three capillary probes. This scheme constituted a true "four-probe" measurement. Cell III had the advantage over Cell II in that the potential circuit was well within the current leads. It was desirable that the potential lead contacts be positioned at least a few millimeters away from and within the current lead contacts, because near the latter the electric field equipotential lines in the specimen are very often not uniform (28). Also, Cell III has exhibited a life in excess of 36 diffusion runs plus calibrations.

Electrical equipment

A partial wiring diagram of the electrical circuit is shown in Figure 4. The system provided for delivering a

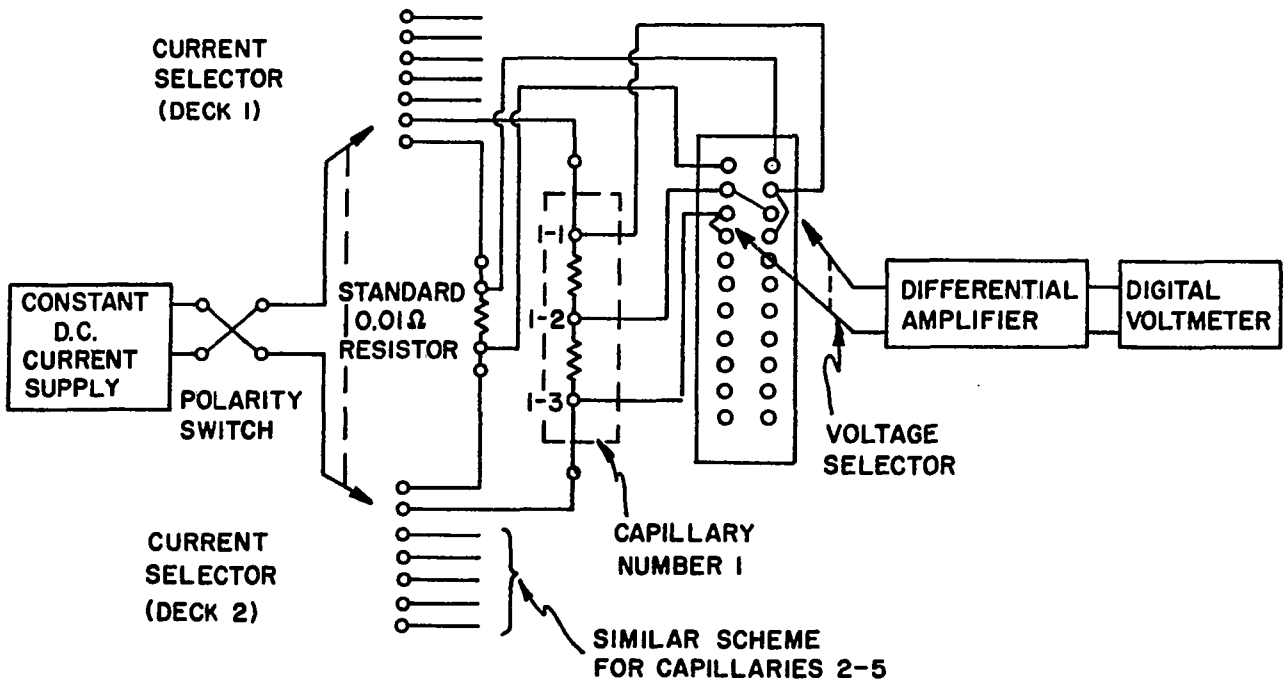

Figure 4. Partial schematic drawing of electrical wiring

constant direct current to any one of the six capillaries and for measuring the voltage drop between any two of the three potential electrodes at each capillary.

The power supply, built by the Ames Laboratory Instrumentation Engineering Group, produced a constant direct current ranging from 0-200 milliamperes. A current of 131 milliamperes (0.17 amp/mm^2) was used. The fluctuation involved with the output current was on the order of 0.001 per cent of the reading. A voltage tap to an internal resistor within the power supply enabled calibration of the D.C. output. Almost no current drift was observed during the two-day diffusion runs. This current then passed through a polarity reversing switch which alternated the current direction every five seconds in order to negate the electrotransport effect in the capillary material. The current was distributed to each capillary by means of a Leeds and Northrup Type 31-3 two-pole rotary selector switch. Also, the current could be passed through a 0.01 ohm Leeds and Northrup standard resistor.

The voltage drop across the various capillary sections was measured on a Hewlett-Packard model 3440A digital voltmeter with a model 3443A high gain/auto range plug-in. Due to the small magnitude (2-5 millivolts) of the potential, the output voltage across the capillary required multiplication by a factor of one hundred through a Hewlett-Packard

8875A differential amplifier.

As there was only a single voltage drop per capillary to be read with the Cell II scheme, one side of the potential circuit for all of the capillaries was wired in common for simplicity. However, it was observed that there was a small amount of current leakage due to this common. On the other hand, the potential circuit for the Cell III scheme utilized a different lead for each electrode which appeared to solve the leakage problem.

Constant temperature apparatus

The diffusion experiments took place in a 7-1/2' x 4' x 3' wooden box lined with one inch thick Styrofoam. A small centrifugal fan distributed the air within the box. Cooling was achieved by circulating tap water in a small heat exchanger attached to the fan output. Attached to the cooler was a two-stage nichrome resistance heater. The temperature controller was a Philadelphia Micro-Set mercury thermo-regulator. A constant temperature of 20-50 °C could be maintained though all experiments were run at 25 °C.

In an attempt to minimize fan vibrations, the fan mounting was isolated from the wooden box with pads of foam rubber and neoprene. In addition, the fan itself was hung from its mounting on springs. The diffusion cell holder was mounted using foam rubber.

Materials

The mercury used in this work was triple cleaned and obtained from the Ames Laboratory. The indium was purchased as 99.999 per cent pure bars from Cominco American Corporation.

Procedure

Before proceeding with a diffusion run the alloy was prepared. Several different procedures were attempted in order to obtain a homogeneous, oxide-free amalgam. In one case the alloy was prepared by mixing liquid mercury and solid indium in a drybox under an argon atmosphere. The mixture was stirred and allowed to remain in the drybox for a half hour. A gray scum, presumed to be oxide, formed on the surface of the amalgam. A similar scum was present when the alloy was prepared in open air. While studying resistivity in the mercury-indium system, Cusack et al. (9) prepared the amalgams under vacuum and in air noticing no difference in the properties measured. At first it was felt that rapid agitation of the mixture immediately prior to a run would produce less oxide in the sample than would be formed by allowing the alloy to sit for a long period of time. Sometimes, however, there appeared to be a non-homogeneous alloy formed. Ultimately it was found that by combining the alloy components without stirring for about two days before a run, homogeneity of the amalgam could be

insured, and the observed oxide formation was about the same as in the short-time agitated preparation. The formation of the gray film appears to be a problem for amalgams less than 10 atomic per cent indium (5), which lies in the range of compositions used in this study. To eliminate the effect of this oxide on the total composition, six times more amalgam was prepared than was needed for a run. Also, it was found that the use of Teflon containers produced less of this scum than when the alloy was prepared in glass beakers since there was less wetting of the Teflon.

Because a single diffusion cell is used for many diffusion runs, it is imperative that it be kept free of dirt and oxide. The Kel-F reservoir and channel sections were cleaned for a short time in nitric acid. It was found that by drawing a knotted thread through the capillaries that the walls could be scraped clean of any residual material. Since this process had the side effect of very slightly enlarging the capillary diameter over a period of time, the cell geometry was recalibrated several times.

The diffusion cell was filled by a technique similar to that used by Powers (33). After the cell was assembled the capillary alloy was poured into the filling hole, flowed into the channel section, and then filled each capillary from bottom to top. After the capillaries were filled, the reservoir and channel sections were rotated isolating

the alloy in the capillary, and the excess material in the channel and reservoir sections was poured out. At this point, in the case of Cell II, the cell was inverted, the channel section was removed, the capillary electrodes were inserted, and the cell was returned to its upright position. For Cells I and III the rotated channel section served as the bottom of each capillary. The reservoirs were then filled with the proper alloy. Subsequent to mounting the cell in the constant temperature apparatus, electrical connections were made to Cells I and III. When thermal equilibrium was reached (about 30 minutes), the reservoir section was rotated to a position such that each reservoir was directly above a capillary thus beginning a run. The start-up process just discussed could be used for cell calibration, resistivity determinations, or diffusion runs.

Before diffusion runs could be made it was necessary to calibrate the cell geometry by determining the effective (A/L) of each of the capillaries. The calibration is made with mercury since its resistivity at 25 °C is well known. This cell factor is found by rearranging Equation 14 to give

$$\left(\frac{A}{L}\right) = \frac{\rho e}{R} . \qquad (16)$$

Further, it was necessary to determine the resistivity-composition relationship for 0.00-13.19 atomic per cent indium in mercury. Although resistivities for this system

were previously reported for the entire composition range by Cusack et al. (9), Roll and Swamy (35), and Schultz (36), few data are available in the small indium composition range required. Also, determining the relationship served as a check on the measuring technique.

In all of the diffusion experiments the denser of the two initial alloys was placed in the capillary. The initial composition differences ranged from 1.72 to 6.79 atomic per cent indium over a composition range of 0.00 to 13.19 atomic per cent indium.

Immediately after the capillary and reservoir were aligned, the voltage drop across the three sections of each of the six capillaries was noted. For each capillary, this process took about 20 seconds. Thus, the current, whose polarity was reversed every five seconds, was itself reversed four times during the capillary voltage measurements. This cancelled out the electrotransport effect. In addition, when readings were not being taken, the current flowed through the standard resistor. Voltage readings, taken about 14 times over a two day interval, could be converted to a resistivity history of the capillary contents. This amounted to current flowing intermittently through the capillary for less than five minutes during an entire run.

An additional problem caused by the presence of an electrical current is the I^2R heating of the capillary

contents. If the capillary material were assumed to be filled with mercury (worst case) and completely insulated (which it is not), a current of 131 milliampheres applied for 20 seconds would cause a temperature rise of less than 0.3 ^{o}C. This rise is negligible with respect to its effect on the diffusion process and would not be a cumulative effect.

The current supply and digital voltmeter could be easily zeroed and calibrated independently. The amplifier, which exhibited the most drift of the components, was then calibrated in relation to the current supply and voltmeter prior to each reading.

When it was desired to halt a run, a final set of voltage readings was taken. There was no further need for a final material analysis of the capillary contents so, any further handling of the diffusion cell caused no problems.

TREATMENT OF DATA

Handling of the data for a diffusion experiment where only the initial and final capillary compositions are known is indeed a straightforward matter. However, when the complete composition history of the capillary material is known, a slightly more complex method of data analysis is required.

For the minimal number of runs made using Cell II, the voltage data were changed to composition data by direct proportion. Thus, the atomic fractions in Equation 11, were simply replaced by voltages, and the diffusion coefficient for each capillary at each data point was determined by an implicit, iterative solution of Equation 17 by truncating the series after the sixteenth term,

$$\overline{\Theta}(t) = \frac{\overline{V}-V_R}{V_o-V_R} = \frac{8}{\pi^2} \sum_{n=0}^{\infty} \left(\frac{1}{2n+1}\right)^2 \cdot \exp\left[\frac{-\pi^2}{4}(2n+1)^2 \frac{Dt}{L^2}\right]. \tag{17}$$

The rationale for this voltage-composition proportionality arose because no resistivity data had been taken at that time, and the data of Cusack et al. (9) was assumed to be linear over the 0-13 atomic per cent indium range. Although it is true that the data of Cusack et al. were scanty in this region the purpose of Cell II was simply to attest to the feasibility of such a measuring technique, and only

approximate results were required. Once the diffusion coefficients were determined at each point, it was noted that there was a substantial degree of variance in the D-values for a single capillary within a run. On the other hand, the definition says that the diffusivity should be independent of time. Therefore, it was decided to determine a least squares fit of the individual capillary data which would produce a single average diffusion coefficient over the entire time range of data. These average values are those diffusion coefficients reported for the Cell II results. It was felt at this point that a resistivity determination of the average composition in the capillary was indeed feasible, but certain deficiencies in the Cell II design mentioned earlier required modification.

Because of the flexible design of Cell III, more precise data analysis was possible than previously. The resistivity data that were taken over the 0-13 atomic per cent indium showed a curvature that could not be detected in the data of Cusack et al. (9). This resistivity-composition relationship was approximated by dividing the curve into five straight line segments. The raw voltages could be converted to resistivities and hence to compositions. Since the electrodes in Cell III were placed at arbitrary points along the capillary length, Equation 13 was used to determine the diffusion coefficients,

$$\tilde{\theta}(t) = \frac{8}{\pi^2} \sum_{n=0}^{\infty} \frac{1}{(2n+1)^2(\beta-\alpha)} \exp\left[\frac{-\pi^2}{4}(2n+1)^2 \frac{Dt}{L^2}\right]$$

$$\left[\cos\frac{\alpha\pi}{2}(2n+1) - \cos\frac{\beta\pi}{2}(2n+1)\right] . \qquad (13)$$

With this cell design three times as much data were generated as were with Cell II since the average composition between the first and second (Section 1), second and third (Section 2), and first and third (Section 3) electrodes was determined. The diffusion coefficient computations were performed in the following order:

1. At the last set of data points taken, the diffusion coefficients for Section 3 are calculated from Equation 13 using the single term truncation of the series as a first estimate.
2. The second and ensuing estimates of D are made using a Newton-Raphson search technique (25) coupled with Equation 13. Since the function involved is quite "well-behaved", usually only three to five iterations are necessary to find D to a tolerance of 2×10^{-8} cm^2/sec.
3. The diffusivity is found for each preceding data point as above until all the values for D for Section 3 of each capillary are known.
4. Using the diffusivity computed at the final data

point for Section 3 of each capillary as a first estimate, compute all the diffusivities of Section 2 in the capillaries as above in steps 2 and 3.

5. Repeat step 4 for Section 1 of each capillary.

The computed D's indicate that there is a greater variance in the diffusion coefficients near the beginning of a run than toward the end of the run. It was decided to fit the last half of the data for each capillary section to obtain a single diffusion coefficient. The reason for using only the last half of the data, that is, those points where $\tilde{\theta} < 0.75$ in Section 3, will be discussed later. Since the data were taken at uneven intervals, a time weighted average of the diffusivity was obtained. With this value, the $\tilde{\theta}$-function of Equation 13 could be determined. To be certain that this function was a least squares best fit of the data, search in both directions about the average D was made. Thus, for each run a total of 18 average diffusion coefficients was computed--six capillaries with three sections each.

Once all the data were gathered, plots for each capillary section relating the average diffusion coefficient to the average of the initial capillary and reservoir composition differences were drawn. A linear regression line and standard error were computed for each. Also a composite regression line and standard error were computed

taking all the runs for a given capillary section as a whole giving three summary values of each.

DISCUSSION AND RESULTS

Equipment Design

Design of the diffusion cell, as stated previously, was an evolutionary process. It was felt that in order for this study to address itself to the general task of liquid metal diffusion measurements, certain problems inherent to both high and low temperature diffusion coefficient determination must be solved. The diffusion cell used by Powers (33) and Wenger (46) certainly demonstrated the advantages of the diffusion apparatus at low and elevated temperatures. If continuous electrical measurement of the composition of the capillary material in this same diffusion cell were to be successful, the probes required positioning which would not affect the diffusion process. Locating the electrodes along the capillary, therefore, proved to be a critical goal. Should the electrode be placed through the capillary wall extending into the capillary, the probe would serve as an obstacle to the diffusion path and complicate the cylindrical geometry of the tube. In the work of Buell and Shuck (3) a 30 mil tungsten electrode was fused into a 1.5 mm I.D. glass tube. Assuming that the electrode protruded to the center of the capillary, the effective area of the capillary was reduced by over one-fifth at each electrode location. The electrodes in Cells I and II were located well out of the

diffusion path, but they presented other problems. The annular electrodes of Cell III not only caused no obstruction in the capillary but also provided for a true "four-probe" measuring system. Moreover, many Cell III electrodes could be located along the capillary length so that a composition profile within the capillary could be determined as well as a composition history.

The Plexiglas used as a container material in the capillary section proved to have several disadvantages. There was difficulty encountered when boring capillary size holes into the Plexiglas-molybdenum laminate. Since molybdenum is much harder than Plexiglas, the metal chips tended to slightly erode the Plexiglas holes on the two ends of the capillary. In addition the softness of Plexiglas will not permit drilling smooth walled capillary holes. This problem was somewhat alleviated with the repeated cleaning of the holes. Using a clear material such as Plexiglas for the purpose of checking hole filling is not necessary since this can better be detected from an electrical continuity check.

Although several cell problems have been noted, it is felt that the final design, Cell III, performed quite adequately and demonstrated the feasibility of an electrical resistivity measuring scheme as applied to the capillary-reservoir diffusion cell.

Resistivity

The results of the resistivity determinations at 25 °C are shown in Figure 5. The data are averages of the resistivities from the 18 capillary sections for each of the compositions. The procedure was the same as for the diffusion runs except that the material in the capillary and reservoir was identical. Comparison has been made with the limited data in this region of Roll and Swamy (35), Cusack et al. (9), and Schultz (36). The Cusack et al. temperature corrections have been applied where the data were at 20 °C. Good agreement is noted in this small composition range. The linear relation between resistivity and composition assumed in the computations for Cell II is evidently in serious error. In diffusion coefficient computations for Cell III the curve in Figure 5 has been approximated by five straight lines in the 0.00-13.19 atomic per cent indium range. These approximations are shown in Table 1. A complete error analysis of the resistivities obtained would be difficult due to the limited amount of data. At the beginning of each diffusion run, however, the initial measured composition of the capillary contents was compared to the weighted alloy composition. Rarely, except in the early runs when the alloy preparation had not yet been finalized and alloy nonuniformity was present, did the measured and weighed alloy differ by more than about 0.3-0.4

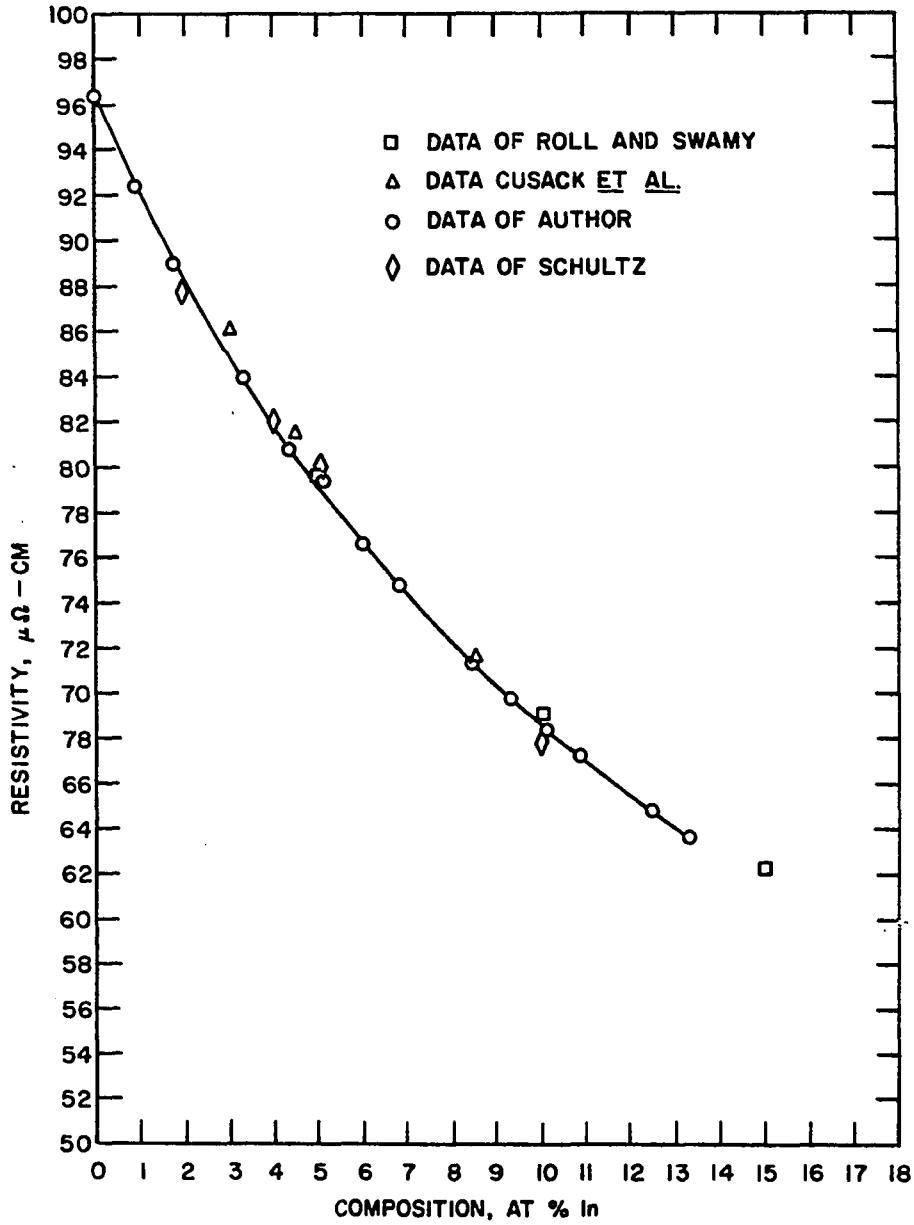

Figure 5. Results of resistivity data obtained in this work at 25 °C compared with the data of other investigators

Table 1. Linear approximations to resistivity data

Line segment	Composition range, at % In	Slope μΩ-cm/at % In	Intercept, μΩ-cm
I	$N_{In} < 2.0$	- 3.895	96.29
II	$2.0 \leq N_{In} < 4.5$	- 3.240	94.98
III	$4.5 \leq N_{In} < 7.0$	- 2.440	91.38
IV	$7.0 \leq N_{In} < 9.5$	- 2.000	88.30
V	$9.5 \leq N_{In} < 13.2$	- 1.572	84.24

per cent of the amount present. This range appears to be an improvement in composition of about threefold over chemical analysis of similar alloys.

Diffusion Coefficients

Cell II

The results of the runs made with Cell II are shown in Table 2. If no value of the diffusivity is reported for a capillary, for example 5-2, this indicates either that the capillary did not fill properly or else that there was some interruption or stoppage in the diffusion process. In several instances it was observed that diffusion would progress normally for a day, and then suddenly there would be no change in composition with time. This was probably

Table 2. Diffusion coefficient calculations for Cell II

Run	Capillary length, cm	Initial comp. diff., at % In	Diffusivity, $cm^2/sec \times 10^5$
5[a]-1[b]	4.58	0-3.443	2.342
5-3	4.62	0-3.443	3.888
5-5	4.61	0-3.443	2.331
5-6	4.62	0-3.443	2.934
6-1	4.58	0-3.443	2.133
6-3	4.61	0-3.443	1.843
6-4	4.64	0-3.443	2.552
6-5	4.61	0-3.443	1.459
6-6	4.61	0-3.443	1.847
7-1	4.58	0-3.443	0.843
7-2	4.63	0-3.443	0.934
7-3	4.61	0-3.443	0.877
7-4	4.64	0-3.443	1.036
7-5	4.61	0-3.443	0.770
7-6	4.61	0-3.443	0.820
8-1	4.57	0-3.443	1.583
8-2	4.61	0-3.443	1.270
8-4	4.64	0-3.443	1.391
8-5	4.62	0-3.443	1.196
8-6	4.62	0-3.443	1.423
9-1	4.57	0-5.127	1.310
9-3	4.62	0-5.127	2.000
9-4	4.64	0-5.127	4.393
9-5	4.62	0-5.127	1.257
9-6	4.63	0-5.127	1.304
10-1	4.58	0-5.127	1.536
10-2	4.63	0-5.127	2.136
10-3	4.61	0-5.127	2.516
10-4	4.64	0-5.127	4.050
10-5	4.61	0-5.127	1.495
10-6	4.61	0-5.127	1.628

[a]Run number.

[b]Capillary number.

Table 2. (Continued)

Run	Capillary length, cm	Initial comp. diff., at % In	Diffusivity, $cm^2/sec \times 10^5$
11-1	4.58	0-5.127	0.978
11-2	4.63	0-5.127	1.190
11-3	4.61	0-5.127	2.901
11-4	4.64	0-5.127	3.186
11-5	4.61	0-5.127	1.891
11-6	4.61	0-5.127	0.823
12-1	2.13	0-5.127	1.609
12-3	2.13	0-5.127	1.836
12-4	2.16	0-5.127	1.958
12-5	2.13	0-5.127	2.183
12-6	2.14	0-5.127	1.822
13-1	4.74	0-5.127	2.863
13-3	4.73	0-5.127	2.863
13-4	4.71	0-5.127	3.212
13-5	4.75	0-5.127	2.968
13-6	4.72	0-5.127	2.848
14-1	4.74	0-3.443	1.633
14-2	4.71	0-3.443	2.762
14-3	4.73	0-3.443	2.504
14-4	4.71	0-3.443	1.807
14-5	4.75	0-3.443	1.912
14-6	4.72	0-3.443	1.582
15-1	4.74	0-6.786	1.798
15-3	4.73	0-6.786	3.877
15-4	4.71	0-6.786	4.867
15-5	4.75	0-6.786	2.251
15-6	4.72	0-6.786	1.065
16-1	4.74	0-6.786	2.359
16-2	4.71	0-6.786	3.015
16-3	4.73	0-6.786	2.468
16-4	4.71	0-6.786	2.276
16-5	4.75	0-6.786	2.209
16-6	4.72	0-6.786	2.269
17-1	4.74	3.443-8.421	1.159
17-2	4.71	3.443-8.421	1.091

Table 2. (Continued)

Run	Capillary length, cm	Initial comp. diff., at % In	Diffusivity, $cm^2/sec \times 10^5$
17-3	4.73	3.443-8.421	1.270
17-4	4.71	3.443-8.421	1.162
17-5	4.75	3.443-8.421	1.141
17-6	4.72	3.443-8.421	1.074

caused by a particle of oxide lodging in the capillary or the formation of an air bubble. A real advantage of the continuous composition monitoring system is evident here. By knowing when the interruption occurred the diffusion coefficient can be calculated for some time prior to this problem. If only the endpoint compositions were known, the apparent diffusivity would be much lower than in reality.

The calculated diffusion coefficients in Table 2 demonstrate a great deal of scatter. These results are summarized in Table 3. Where there have been several replications, the standard deviations are high indicating scatter. However, the capillaries within a run are generally bunched closer than this. This could point up two possible problems: 1) the inability to accurately prepare a known amalgam, or 2) a systematic error in the procedure or equipment design. It is felt that probably both of these situations added to

Table 3. Summary of diffusion coefficient results for Cell II

Initial comp. diff., at % In	Average D, $cm^2/sec \times 10^5$	Std. dev. D, $cm^2/sec \times 10^5$	No. of points
0-3.443	1.756	0.764	26
0-5.127	2.176	0.913	27
0-6.786	2.496	1.098	11
3.443-8.421	1.150	0.069	6

the lack of reproducibility. On the other hand, there are some indications from the range of the data that this general method may be of value. By improving the alloy preparation procedure from the standpoint of precision and homogeneity, significantly less scatter should be evident. Also, the true "four-probe" resistance measurement of Cell III might improve the systematic equipment problems. It should also be repeated here that the incorrect linear composition-resistivity relation was used in all of the Cell II computations.

Cell III

Figure 6 shows a typical plot of the composition history in a capillary for each capillary section of Cell III. On each curve the dashed line depicts the least squares fit of the data based on a time weighted average of the diffusivities computed at each data point for $\tilde{\theta} < 0.75$ in the

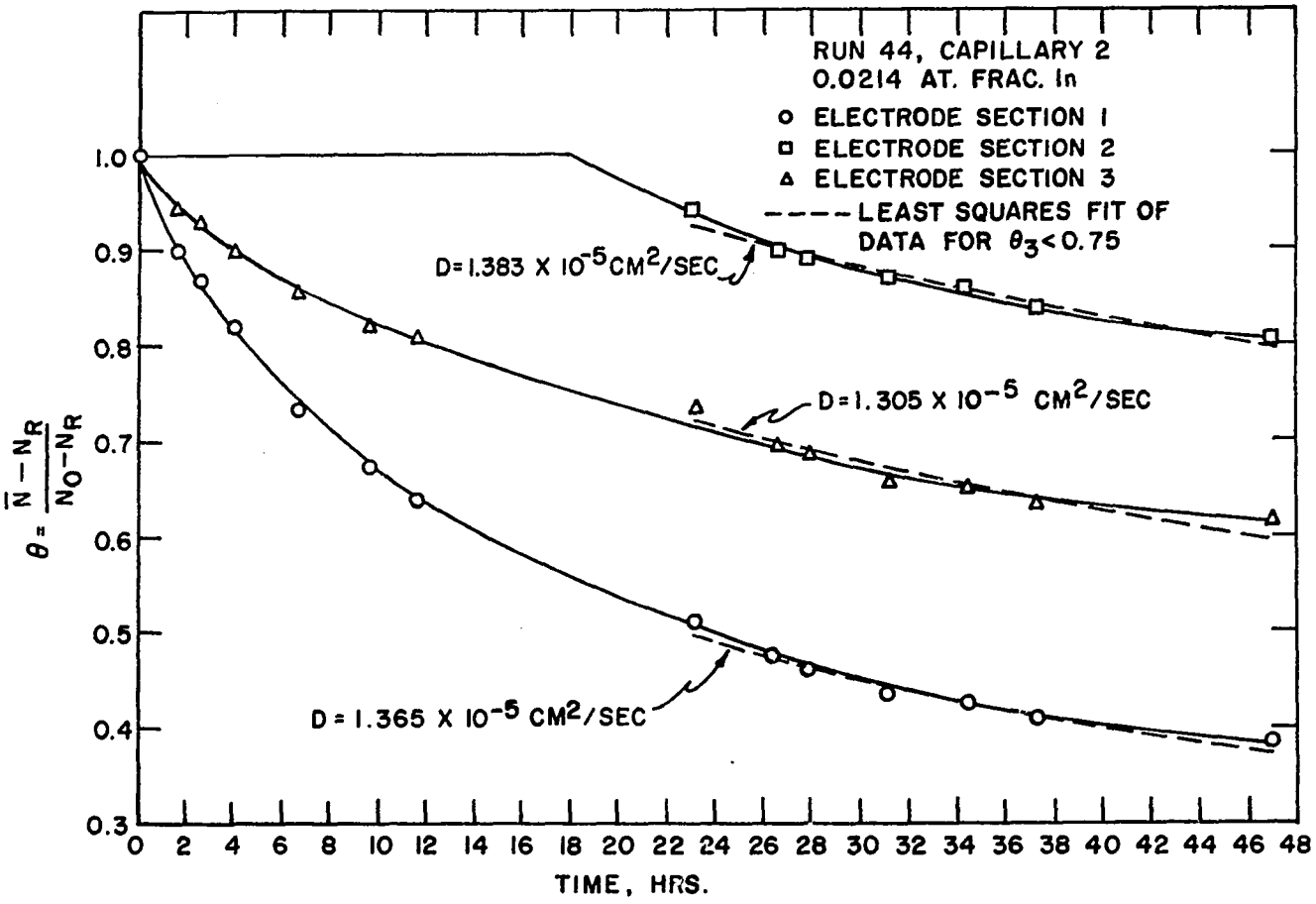

Figure 6. Composition history of a typical capillary

third capillary section (between the top and bottom electrodes). Where $\tilde{\theta} < 0.75$ is tantamount to saying time greater than one day in most cases. It was observed that the diffusivities computed at the earlier data points exhibited a greater degree of fluctuation than those during the second half of a run. It is proposed that the reason for these differences stem from the initial convection induced on start-up. By rotating the reservoir over the capillary at the beginning of a run a degree of mixing of the capillary and reservoir contents is encountered. In addition, the mere handling of the diffusion cell at this point causes some vibration that could enhance this initial convective mixing. Analysis of this problem from the standpoint of diffusate flowing out of the capillary is made. At first this mixing causes a "burst" of diffusate out of the capillary noticed only near the capillary mouth. This burst is not immediately apparent in the rest of the capillary due to the large aspect ratio (L/D) of the capillary of about 50. The original reason for using a capillary geometry is to minimize the effects of convection, and these tend to be damped out in a long, small diameter tube. However, a burst of diffusate from the open end of the capillary must eventually be accounted for in a material balance throughout the capillary. After diffusate material has left a small section near the open end, a material

"void" has been produced in this short length, and a step change in composition is seen between this length and the balance of the capillary. This new dissimilar composition boundary tends to enhance the apparent diffusion coefficient in the balance of the capillary length. Because of the large aspect ratio the effect of the original convective disturbance would take a long time to be noticed near the bottom of the capillary. The experimental data show that there is no appreciable composition change in Section 2 (the lower electrode section) until 18-20 hours have passed. This fact would tend to suggest that the data should be analyzed after about one day of run time to escape the problems associated with start-up induced convection. This, then, is the argument behind fitting the data only after $\tilde{\theta} < 0.75$ in Section 3.

The results of diffusion coefficients generated by experiments with Cell III are shown in Table 4. These data cover a range up to 13.19 atomic per cent indium in the reservoir. In the instance when the results of a run have been deleted, there was reason to believe that the alloys in the cell were not homogeneous. This fact would be evident for the case of the capillary contents from the initial voltage readings. It should be added that these problems were solved with an improved alloy preparation technique after Run 30.

Table 4. Diffusion coefficient calculations for Cell III

Run number	18	21	22	24	26	27	28	29
Composition[a]	0.0256	0.0799	0.0427	0.0552	0.0300	0.0511	0.0758	0.0799
Capillary section	Diffusion coefficient, $cm^2/sec \times 10^5$							
1-1	2.123	1.906	1.519	2.438	1.653	1.664	1.811	1.441
1-2	1.810	1.679	1.632	1.718	1.458	1.708	1.830	1.569
1-3	1.713	1.571	1.375	1.842	1.411	1.456	1.547	1.446
2-1	2.327	2.151	1.613	2.433	1.663	1.466	1.589	1.826
2-2	1.716	1.637	1.555	1.739	1.415	1.678	1.730	1.618
2-3	1.712	1.607	1.393	1.868	1.427	1.440	1.502	1.673
3-1	2.954	1.808	1.831	3.670	1.328	1.324	1.468	1.482
3-2	1.575	1.713	1.581	1.625	1.501	1.694	1.968	1.777
3-3	1.699	1.540	1.316	1.903	1.334	1.389	1.522	1.667
4-1	2.187	2.031	1.418	2.307	1.682	1.499	1.663	1.744
4-2	1.800	1.673	1.494	1.843	1.515	1.733	1.927	1.855
4-3	1.673	1.563	1.224	1.825	1.346	1.390	1.615	1.749
5-1	2.291	2.490	1.951	2.373	1.936	1.349	0.854	1.400
5-2	1.700	1.508	1.373	1.790	1.698	1.608	1.906	1.720
5-3	1.621	1.375	1.252	1.780	1.706	1.316	1.173	1.403
6-1	2.069	2.234	1.849	3.069	-	1.466	1.797	1.423
6-2	1.703	1.525	1.602	1.610	-	1.774	1.912	1.775
6-3	1.570	1.512	1.406	1.737	-	1.491	1.682	1.666

[a]Average of initial capillary and reservoir compositions, at. frac. In.

Table 4. (Continued)

Run number	31	32	33	34	35	36	37	38
Composition[a]	0.0879	0.0677	0.1002	0.0172	0.0386	0.0215	0.0719	0.1161
Capillary section	Diffusion coefficient, $cm^2/sec \times 10^5$							
1-1	1.374	1.161	2.205	1.043	0.871	0.908	1.570	1.323
1-2	1.626	1.893	1.627	1.323	1.782	1.556	1.733	1.991
1-3	1.326	1.428	1.343	1.093	1.267	1.215	1.830	1.679
2-1	1.404	1.221	1.286	1.179	1.299	1.187	1.829	1.477
2-2	1.586	1.888	1.617	1.163	1.816	1.567	1.647	2.316
2-3	1.297	1.462	1.231	1.114	1.572	1.306	1.620	1.853
3-1	1.428	1.371	1.343	0.802	1.144	1.562	1.049	1.236
3-2	1.638	1.795	1.540	1.278	1.858	1.514	1.934	1.940
3-3	1.349	1.499	1.253	0.982	1.483	1.301	1.550	1.564
4-1	1.552	1.522	1.497	-	1.285	1.565	1.603	1.491
4-2	1.665	1.857	1.642	-	1.866	1.617	1.729	1.863
4-3	1.360	1.517	1.302	-	1.598	1.360	1.619	1.582
5-1	1.388	1.423	1.336	-	1.215	1.262	1.415	1.659
5-2	1.595	1.859	1.620	-	1.812	1.575	1.646	1.786
5-3	1.347	1.530	1.260	-	1.553	1.314	1.598	1.661
6-1	1.550	1.598	1.313	1.185	1.756	2.180	2.203	1.518
6-2	1.602	1.907	1.621	1.086	1.850	1.459	1.672	1.741
6-3	1.366	1.567	1.234	0.978	1.749	1.422	1.860	1.636

Table 4. (Continued)

Run number	39	40	41	42	43	44	45	46
Composition[a]	0.0882	0.0343	0.0595	0.1082	0.0258	0.0214	0.0129	0.0759
Capillary section	Diffusion coefficient, $cm^2/sec \times 10^5$							
1-1	1.327	1.337	1.342	1.497	1.363	1.365	1.144	1.133
1-2	1.785	1.743	1.759	1.881	1.628	1.279	-	1.693
1-3	1.827	1.612	1.577	1.763	1.499	1.268	1.208	1.234
2-1	1.730	1.209	1.609	1.986	1.268	1.365	1.969	1.700
2-2	1.801	1.633	1.796	1.582	1.594	1.383	0.934	1.443
2-3	1.675	1.600	1.731	1.817	1.310	1.305	1.021	1.246
3-1	1.303	1.575	1.902	1.446	1.116	1.232	1.111	1.098
3-2	1.904	1.569	1.578	1.829	1.645	1.356	1.028	1.736
3-3	1.632	1.685	1.622	1.598	1.317	1.248	1.005	1.197
4-1	1.659	1.461	1.527	1.833	1.421	1.455	1.383	1.353
4-2	1.548	1.613	1.673	1.707	1.757	1.014	-	1.632
4-3	2.114	1.635	1.538	1.731	1.496	1.120	0.940	1.221
5-1	1.338	1.570	1.424	1.562	1.757	1.705	1.196	1.274
5-2	1.925	1.628	1.698	1.760	1.621	-	-	1.566
5-3	1.718	1.661	1.556	1.694	1.464	-	-	1.156
6-1	1.980	1.632	1.858	1.755	1.911	1.686	1.863	1.250
6-2	1.639	1.660	1.892	1.857	1.620	1.335	2.014	1.760
6-3	1.782	1.677	1.811	1.851	1.486	1.411	1.829	1.231

Table 4. (Continued)

Run number	47	48	49	50	51	52	53	54
Composition[a]	0.0841	0.0922	0.0427	0.0173	0.1121	0.0339	0.1080	0.0839
Capillary section	Diffusion coefficient, $cm^2/sec \times 10^5$							
1-1	1.864	1.390	0.885	1.206	2.160	1.314	1.567	1.522
1-2	1.820	2.033	1.434	1.649	1.720	1.380	1.730	1.753
1-3	1.912	1.670	0.839	1.358	1.641	1.115	1.553	1.422
2-1	1.519	1.633	1.010	1.369	1.801	1.178	1.754	1.352
2-2	1.762	1.858	1.401	1.289	1.760	1.452	1.745	1.714
2-3	1.741	1.730	0.928	1.433	1.550	1.063	1.556	1.433
3-1	1.686	1.417	1.017	1.382	1.487	1.218	1.360	1.467
3-2	1.790	1.840	1.369	1.639	1.830	1.417	1.677	1.715
3-3	1.873	1.695	0.932	1.436	1.506	1.179	1.330	1.408
4-1	1.418	1.546	0.943	1.241	1.846	1.254	1.647	1.554
4-2	1.975	2.029	1.456	2.057	1.746	1.190	1.829	1.695
4-3	1.766	1.786	0.875	1.545	1.497	1.016	1.510	1.408
5-1	1.460	1.335	0.999	1.366	1.405	1.252	1.356	1.464
5-2	1.805	1.726	1.384	1.825	1.710	1.387	1.687	1.636
5-3	1.728	1.556	0.904	1.453	1.393	1.157	1.413	1.341
6-1	1.496	1.852	1.058	1.693	1.954	2.127	1.915	1.543
6-2	1.772	1.740	1.413	1.846	1.473	1.338	1.947	1.762
6-3	1.655	1.741	0.926	1.568	1.405	1.284	1.713	1.446

After the composition versus diffusion coefficient data were gathered, a scatter plot was made for each capillary section. These plots are shown in Appendix B. A linear regression model of the data was assumed, and these results are summarized in Table 5. Table 6 combines all the data of Table 5 from Sections 1, 2, and 3 respectively. In addition, Figure 7 shows a composite plot of the results from Section 2. Since gross errors in diffusion measurements as a result of excessive vibration are usually manifested as very high values of D, these values have been omitted in the regression estimations of Tables 5 and 6.

Both the plots and the magnitude of the standard errors of the estimate indicate some scatter of the data about the regression line. There appears to be considerably less scatter about the regression line for Cell III than there is about the means of Cell II. One can conclude, then, that Cell III is superior to Cell II from a reproducibility standpoint. This result was not wholly unexpected due to the improved equipment.

It is felt that the diffusivities determined in Section 1 (top two electrodes) are the least reliable of the three capillary measurements. This portion of the capillary is most plagued by problems associated with the capillary mouth region. The buildup of diffusate due to a lack of stirring and a ΔL effect, that is, effectively shortening of the

Table 5. Regression values from Cell III data

Capillary section	Slope[a]	Intercept, $cm^2/sec \times 10^5$	Corr. coef.	Std. error $cm^2/sec \times 10^5$
1-1	4.603	1.168	0.426	0.324
1-2	3.361	1.473	0.596	0.145
1-3	3.845	1.234	0.497	0.219
2-1	3.766	1.285	0.432	0.260
2-2	3.979	1.360	0.587	0.173
2-3	3.767	1.245	0.491	0.218
3-1	2.037	1.239	0.265	0.244
3-2	4.471	1.378	0.682	0.156
3-3	2.881	1.261	0.391	0.221
4-1	3.447	1.299	0.523	0.182
4-2	2.473	1.541	0.341	0.213
4-3	3.579	1.257	0.417	0.250
5-1	- 0.626	1.456	- 0.084	0.243
5-2	1.325	1.587	0.278	0.141
5-3	0.694	1.405	0.099	0.215
6-1	- 0.531	1.727	- 0.060	0.298
6-2	1.847	1.559	0.288	0.200
6-3	1.693	1.433	0.228	0.236

[a]In $cm^2/(sec - at\ frac\ In) \times 10^5$.

Table 6. Summary of regression values for the three capillary sections

Capillary section	Slope[a]	Intercept, $cm^2/sec \times 10^5$	Corr. coef.	Std. error $cm^2/sec \times 10^5$
1	2.195	1.355	0.241	0.283
2	3.004	1.475	0.471	0.175
3	2.800	1.301	0.363	0.226

[a] In $cm^2/(sec\text{-}at\ frac\ In) \times 10^5$.

capillary due to an excess of stirring of the reservoir material are two of these problems. Since no mechanical stirring is used, the stagnation of diffusate in the region of the capillary mouth is probably a factor in these experiments. Zavadoski (48) has shown numerically that this build-up has a significant effect on D when short capillaries are used. Although the intercept is comparable, the slope of the diffusion coefficient-composition line for Section 1 in Table 6 is less than that for Section 2 or 3. This would lend credence to the idea of a stagnation at the mouth seriously affecting diffusion in Section 1. Electrodes 5-1 and 6-1 in Table 5 even show a small negative slope. Moreover, the larger standard error would cast further doubt on the data reliability in this region.

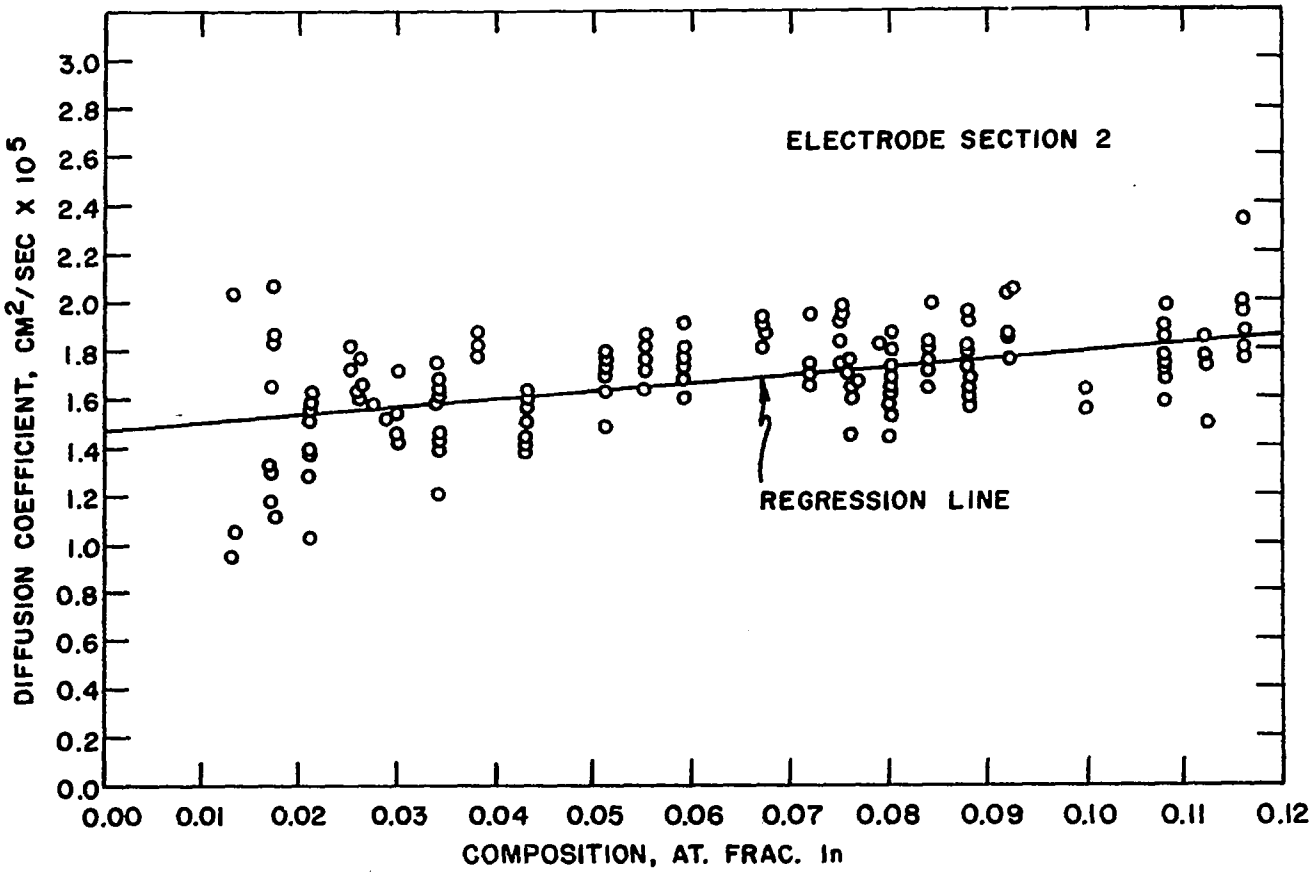

Figure 7. Composite diffusion coefficient results from Section 2

Comparison with previous work

The composite regression line for Section 2 is plotted in Figure 8 along with the data of Nanda and Shuck (31) and Equation 3 developed by Darken (10). The Equation 3 graph may suffer from an inability to estimate the proper D* values. The assumptions made in the Darken analysis are as follows:

1) The D* function is linear.
2) $D_{Hg-HgT} = 1.75 \times 10^{-5}$ cm^2/sec from Broome and Walls (2).
3) $D_{In-InT} = 4.6 \times 10^{-6}$ cm^2/sec from Careri et al. (6) extrapolated to 25 °C.
4) $D_{In-HgT} = D_{In-InT} \left(\frac{r_{In}}{r_{Hg}}\right)$ from the Stokes-Einstein equation (15).
5) $D_{Hg-InT} = 1.4 \times 10^{-5}$ cm^2/sec from intercept of author's data.

D^*_{In}, then, was found by drawing a straight line from D_{Hg-InT} to D_{In-InT}, and D^*_{Hg} was taken as a linear function between D_{In-HgT} and D_{Hg-HgT}. The activity data of Butler (5) was also used in the computation. There appears to be reasonable agreement with the experimental data of Nanda and Shuck (31) with regard to slope, but their intercept is somewhat lower. While each of the relations shows an increase in the diffusion coefficient with composition, the Darken equation (10) is quite dependent on the evaluation of the parameters

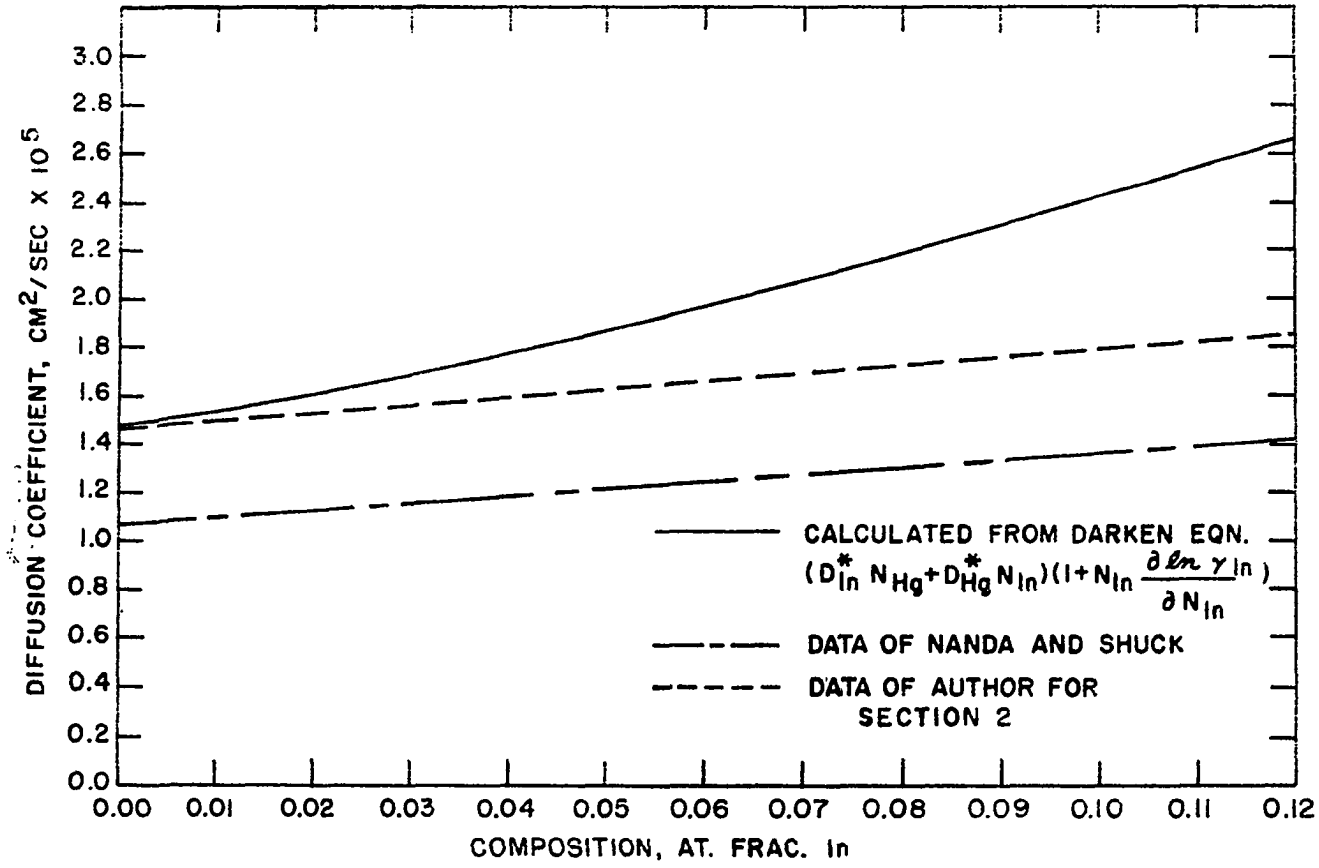

Figure 8. Comparison of the results obtained in this work with the Darken equation and the data of Nanda and Shuck

required to determine D*.

There has been little experimental work, in general, which attempts to study liquid metal diffusion coefficients as a function of composition. Rather, most of the work has involved a temperature correlation of diffusivity using small amounts of solute in the liquid system. Table 7 shows the results of some solute diffusion studies in the indium-mercury system. The data of this work for dilute indium

Table 7. Comparison of In-Hg diffusion coefficients with other investigators using low indium composition alloys

Temp., °C	Diffusion coefficient $cm^2/sec \times 10^5$	Investigator
25	1.79	Butler and Shuck (4)
25	1.38	Mangelsdorf (26)
25	1.10[a]	Nanda and Shuck (31)
25	1.70	Powers (33)
22	1.47	Stackelberg and Toome (37)
25	1.31	Stromberg and Zakharova (40)
25	1.36[a]	This work Section 1
25	1.48[a]	This work Section 2
25	1.30[a]	This work Section 3

[a]Extrapolated to 0.00 at frac. In.

amalgams fall well within the range of diffusivities previously reported for this alloy.

Evaluation of the Technique

The errors associated with any diffusion determination include the measurement of time, geometric parameters, and composition in addition to the degree of constancy of controlled variables such as vibration and temperature. Of these, the most difficult obstacle is composition measurement. In the capillary-reservoir system it is desirable to measure at least the initial and average compositions of the capillary material for each value of the diffusivity. Moreover, a ratio of composition differences is required in the computation of D. Thus, the composition measurement becomes a very sensitive function of the diffusion coefficient. The main goal of this project was to arrive at an improved composition measurement without the side effect of disturbing the actual diffusion process.

Previously, chemical analyses on similar alloys were accurate to within one to two per cent of the total amount present. This obviously has a serious effect on the diffusion coefficient calculation since initial composition differences of only 5 to 10 per cent were used. With Cell III, however, it is possible to determine compositions based on resistivity measurements (as discussed in the resistivity results) to within 0.3-0.4 per cent of the amount present.

This, in effect, is an improvement of a factor of two or three over a chemical analysis. The error in D caused by time, geometry, and temperature is, however, still negligible compared to that caused by composition determination. If the error is roughly analyzed on the basis of Equation 12, the 0.4 per cent error in composition for a 3 per cent initial composition difference will cause a 16 per cent error in D while a 0.002 cm error in the capillary length will add an additional 2 per cent error. This amounts to an 18 per cent known error in the diffusivity. On the other hand, there was a substantial vibration error within the laboratory. The value of this is hard to assess, but vibration measurements taken in the room after experimentation indicated that this could have added to the error.

Cell III offers a number of advantages including a saving of time. The voltage data can quickly be referred to compositions and the diffusion coefficient immediately computed as opposed to the laborious, less accurate chemical analysis. Errors associated with the melting-solidification cycle are evaded since the final material analysis (as well as all others) is made in situ. The continuous composition determination offers a complete composition history of the capillary material rather than simply two endpoints. Moreover, if a problem occurs such as a blockage in the capillary due to an oxide particle or a gas bubble, the

monitoring system can locate both where and when the obstruction occurred. Knowing this, the data can be salvaged, and the diffusivity can be computed for some earlier time interval. The system enables diffusion studies for very small initial composition differences of about two atom per cent indium. This is important to the assumption of a constant diffusivity in Fick's Second Law. In general, this scheme has encompassed the advantages of the capillary-reservoir system with the convenience and added knowledge of continuous monitoring.

SUMMARY AND RECOMMENDATIONS

A capillary-reservoir diffusion cell has been designed to follow the liquid metal diffusion process in a capillary on a continuous basis. Electrical probes were placed in the capillary so that the composition change could be monitored by noting the change in resistivity of the capillary material between probes. Molybdenum sheet electrodes were laminated between layers of Plexiglas such that when capillary holes were drilled into the composite, the electrodes placed at various distances along the capillary were in the form of annuli. This probe configuration enabled the measurement of voltages (resistances) without disturbing the actual diffusion process. Composition dependence of the diffusion coefficient in the mercury-indium system was studied at 25 ^{o}C for compositions up to 13.19 atomic per cent indium. This amalgam proved desirable since it has a wide liquid range at room temperature, and small composition changes in this range are reflected by large changes in resistivity.

When compared to similar previous data, the results indicate that the technique is quite adequate. The summary linear regression equations for two electrode sections (in cm^2/sec) are as follows:

Section 2. $D = 3.00 \times 10^{-5} \bar{N} + 1.48 \times 10^{-5}$ (18)

Section 3. $D = 2.80 \times 10^{-5} \bar{N} + 1.30 \times 10^{-5}$. (19)

It is felt that this apparatus should in the future be applied to diffusion measurements at elevated temperatures assuming that a suitable electrically nonconductive container material could be found in place of Plexiglas. A product like Lavite or other ceramic might be such a material. The electrode must, of course, be nonreactive with respect to either component of the binary. A combination of the Wenger (46) cell and that used in this work should prove acceptable.

The actual measurement of the potential drop between electrodes was adequate for this work, but an improvement should be made in the amplifier circuit to minimize drift. A voltmeter capable of directly reading the small potentials involved without amplification would be better yet.

Finally, it should be realized that the resistivity determination of composition is only possible for binaries whose constituents have considerably differing resistivities. There are numerous liquid metal systems to which this scheme cannot apply.

NOMENCLATURE

A	cross sectional area, cm^2
C	composition, arbitrary units
D	diffusion coefficient, cm^2/sec
D_i^*	diffusion coefficient of i determined by a tracer technique in an alloy of the same composition, cm^2/sec
D_o	Arrhenius frequency factor, cm^2/sec
I	current, amperes
L	capillary length, cm
N	composition, atom fraction
Q_o	Arrhenius activation energy, kcal/mole
R	resistance, ohms
t	time, sec
V	potential difference, millivolts
x	distance along capillary, cm
α	fraction of capillary length
β	fraction of capillary length
γ_i	activity coefficient of i
θ	dimensionless composition
ρ	density, g/cm^3
ρ_e	electrical resistivity, $\mu\Omega$-cm

Subscripts

o	initial property at t = 0
R	reservoir property

Superscript

T tracer

Diacriticals

$\bar{}$ average property between 0 and L

$\tilde{}$ average property between αL and βL

BIBLIOGRAPHY

1. Anderson, J. S. and Saddington, K. The use of radioactive isotopes in the study of the diffusion of ions in solution. Journal of the Chemical Society Suppl. 2: S381. 1949.

2. Broome, E. F. and Walls, H. A. Liquid metal diffusion: a modified shear cell and mercury diffusion measurements. Metallurgical Society of AIME Transactions 242: 2177. 1968.

3. Buell, C. H. and Shuck, F. O. Diffusion in the liquid Bi-Sn system. Metallurgical Transactions 1: 1875. 1970.

4. Butler, F. E. and Shuck, F. O. Diffusion in the indium-mercury system. Metallurgical Society of AIME Transactions 245: 3. 1969.

5. Butler, J. N. Activity coefficients of liquid indium-mercury at 25°. Journal of Physical Chemistry 68: 1828. 1964.

6. Careri, G., Paoletti, A., and Salvetti, F. L. Self diffusion in liquid indium. Nuovo Cimento 10: 399. 1954.

7. Castleman, A. W., Jr. Diffusion in liquid metal systems. Unpublished Ph.D. thesis. New York, New York, Library, Polytechnic Institute of Brooklyn. 1969.

8. Cooper, C. W. and Furman, N. H. The diffusion coefficients of certain metals in mercury. Journal of the American Chemical Society 74: 6183. 1952.

9. Cusack, N., Kendall, P., and Fielder, M. Electron transport properties in a liquid alloy. Philosophical Magazine 10: 871. 1964.

10. Darken, L. S. Diffusion, mobility, and their interaction through free energy in binary metallic systems. Metallurgical Society of AIME Transactions 175: 184. 1948.

11. Davis, K. G. and Fryzuk, P. Diffusion of silver in liquid tin. Metallurgical Society of AIME Transactions 233: 1662. 1965.

12. Edwards, J. B., Hucke, E. E., and Martin, J. J. Diffusion in binary liquid metal systems. Metals and Materials 2, No. 2, Metallurgical Reviews 13, No. 120: 1. 1968.

13. Edwards, J. B., Hucke, E. E., and Martin, J. J. The measurement of diffusion coefficients in binary liquid metals with a concentration cell. Electrochemical Society Journal 115: 488. 1968.

14. Ehrenberg, W. Electrical conduction in semiconductors and metals. London, England, Oxford Press. 1958.

15. Frenkel, J. Kinetic theory of liquids. New York, New York, Dover Publications. 1958.

16. Glasstone, S., Laidler, K. J., and Eyring, H. The theory of rate processes. New York, New York, McGraw-Hill Book Company, Inc. 1941.

17. Grace, R. E. and Derge, G. Diffusion in liquid lead-bismuth alloys. Metallurgical Society of AIME Transactions 203: 839. 1955.

18. Gupta, Y. P. and Wang, H. S. Diffusion of zinc and germanium in liquid silver. Metallurgical Society of AIME Transactions 245: 619. 1969.

19. Hesson, J. C. and Burris, L. Uranium diffusivity in cadmium. Metallurgical Society of AIME Transactions 227: 571. 1963.

20. Hoffman, R. E. The self-diffusion of liquid mercury. The Journal of Chemical Physics 20: 1567. 1952.

21. Kawalki, W. Untersuchungen uber die Diffusionsfahigkeit einiger Electrolyte in Alkohol. Ein Beitrag zur Lehre von der Constitution der Lesungen. Annalen der Physik und Chemie 52: 166. 1894.

22. Leak, V. G. and Swalin, R. A. Diffusion of silver and tin in liquid silver. Metallurgical Society of AIME Transations 230: 426. 1964.

23. Ma, C. H. and Swalin, R. A. A study of solute diffusion in liquid tin. Acta Metallurgica 8: 388. 1959.

24. Ma, C. H. and Swalin, R. A. Self diffusion in liquid tin. The Journal of Chemical Physics 36: 3014. 1962.

25. McCracken, D. D. and Dorn, W. S. Numerical methods and Fortran programming. New York, New York, John Wiley and Sons, Inc. 1964.

26. Mangelsdorf, P. C. Electrolysis and diffusion in liquid alloys. In St. Pierre, George, R., editor. Physical Chemistry of Process Metallurgy. Part 1. P. 429. New York, New York, Interscience Publishers. 1961.

27. Mangelsdorf, P. C. Transport process in liquid alloys. I. A transport cell for liquid alloys. Journal of Chemical Physics 30: 1170. 1959.

28. Meaden, G. T. Electrical resistance in metals. New York, New York, Plenum Press. 1965.

29. Mirshamsi, M., Cosgarea, A., Jr., and Upthegrove, W. R. Self diffusivities of cadmium and lead in the binary-liquid cadmium-lead system. Metallurgical Society of AIME Transactions 236: 122. 1966.

30. Nachtrieb, N. H. and Petit, J. Self diffusion in mercury. Journal of Chemical Physics 24: 746. 1956.

31. Nanda, A. K. and Shuck, F. O. Diffusion in In-Hg amalgams. Metallurgical Transactions 1: 353. 1970.

32. Niwa, K., Shimoji, M., Kado, S., Watanabe, Y., and Yokokawa, T. Studies on diffusion in molten metals. Metallurgical Society of AIME Transactions 209: 96. 1957.

33. Powers, J. R. Convection in capillary measurements. Unpublished M.S. thesis. Ames, Iowa, Library, Iowa State University. 1968.

34. Roberts-Austen, W. C. On the diffusion of metals. Proceedings of the Royal Society of London 59: 281. 1896.

35. Roll, A. and Anantha Swamy, N. K. Die elektrische Widerstand von metallischen Schmelzen. Zeitschrift für Metallkunde 52: 111. 1961.

36. Schultz, L. G. The experimental study of the optical properties of metals and the relation of the results to the Drude free electron theory. Advances in Physics 6: 102. 1967.

37. Stackelberg, M. and Toome, V. Bestimmung einiger Diffusion-koeffizienten von Metallen in Quecksilber mit Hilfe der Amalgam-Tropfelektrode. Zeitschrift fur Electrochemie 58: 226. 1954.

38. Stahlhut, D. P. Liquid metal convection in small capillaries. Unpublished M.S. thesis. Ames, Iowa, Library, Iowa State University. 1969.

39. Steel, R. G. D. and Torrie, J. H. Principles and procedures of statistics. New York, New York, McGraw-Hill Book Company, Inc. 1960.

40. Stromberg, A. G. and Zakharova, E. A. Diffusion constants of metals in mercury. Soviet Elektrokhimiya 1: 922. 1965.

41. Sutherland, W. A dynamical theory of diffusion for nonelectrolytes and the molecular mass of albimin. Philosophical Magazine 9: 781. 1905.

42. Swalin, R. A. On the theory of self-diffusion in liquid metals. Acta Metallurgica 7: 736. 1959.

43. Verhoeven, J. D. Convection effects in the capillary-reservoir technique for measuring liquid metal diffusion coefficients. Metallurgical Society of AIME Transactions 242: 1937. 1968.

44. Walls, H. A. and Upthegrove, W. R. Theory of liquid diffusion phenomena. Acta Metallurgica 12: 461. 1964.

45. Weischedel, F. Zur Diffusion von Metallen in Quecksilber. Zeitschrift fur Physik 85: 29. 1933.

46. Wenger, J. C. Determination of diffusion coefficients in a liquid In-Sn system. Unpublished M.S. thesis. Ames, Iowa, Library, Iowa State University. 1969.

47. Widder, D. V. Advanced calculus. 2nd ed. Englewood Cliffs, New Jersey, Prentice-Hall Inc. 1961.

48. Zavadoski, R. W. Analysis of convection effects in capillary-reservoir diffusion measurements. Unpublished Ph.D. thesis. Ames, Iowa, Iowa State University. 1970.

ACKNOWLEDGMENTS

The author wishes to express his gratitude to Dr. Frank O. Shuck for his guidance and encouragement during the course of this project. In addition, the assistance of Harvey Jensen and the Ames Laboratory Research Shop during the equipment construction is appreciated. Finally, thanks are extended to my wife, Pauline, for her patience and understanding throughout the disappointments and successes of this work.

APPENDIX A

Determination of Average Capillary Composition

The method of separation of variables yields the well known equation

$$\theta(x,t) = \frac{N-N_R}{N_o-N_R} = \frac{4}{\pi} \sum_{n=0}^{\infty} \left(\frac{1}{2n+1}\right) \exp\left[\frac{-\pi^2}{4}(2n+1)^2 \frac{Dt}{L^2}\right] \sin\left[\frac{\pi}{2L}(2n+1)\,x\right] . \qquad (12)$$

This equation can be integrated to find the average composition between any two arbitrary points in the capillary, αL and βL, as shown in the following diagram:

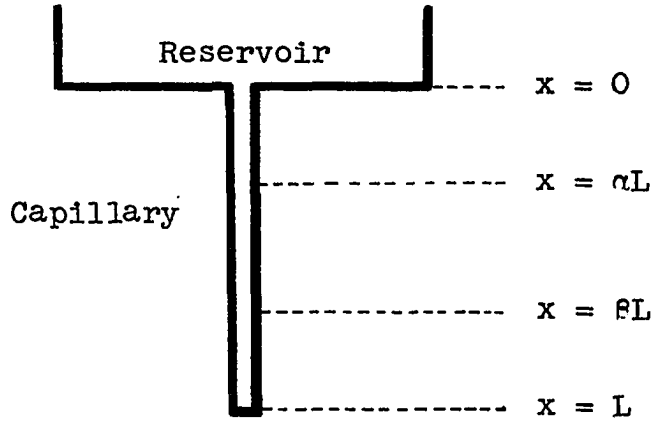

where

α and β are fractions of the total length $0 \leq \alpha < \beta \leq L$.

$$\tilde{\theta}(t) = \frac{\tilde{N}-N_R}{N_o-N_R} = \frac{\int_{\alpha L}^{\beta L} \theta(x,t)dx}{\int_{\alpha L}^{\beta L} dx} . \qquad (20)$$

$$\tilde{\theta}(t) = \frac{\frac{4}{\pi}\int_{\alpha L}^{\beta L}\sum_{n=0}^{\infty}\left(\frac{1}{2n+1}\right)\exp\left[\frac{-\pi^2}{4}(2n+1)^2\frac{Dt}{L^2}\right]\sin\left[\frac{\pi}{2L}(2n+1)x\right]dx}{\beta L - \alpha L}.$$

(21)

It can be shown with the aid of Weierstrass's M-test (47) that the series in the numerator of Equation 21 is uniformly convergent on at least the interval [αL, βL]; thus, the series can be integrated term by term as

$$\tilde{\theta}(t) = \frac{4}{\pi(\beta-\alpha)L}\sum_{n=0}^{\infty}\int_{\alpha L}^{\beta L}\left(\frac{1}{2n+1}\right)\exp\left[\frac{-\pi^2}{4}(2n+1)^2\frac{Dt}{L^2}\right]$$

$$\sin\left[\frac{\pi}{2L}(2n+1)x\right]dx\ . \qquad (22)$$

It is convenient here to define $Z_n \neq Z_n(x)$ as

$$Z_n = \left(\frac{1}{2n+1}\right)\exp\left[\frac{-\pi^2}{4}(2n+1)^2\frac{Dt}{L^2}\right]. \qquad (23)$$

Equation 22 then becomes

$$\tilde{\theta}(t) = \frac{4}{\pi(\beta-\alpha)L}\sum_{n=0}^{\infty} Z_n \int_{\alpha L}^{\beta L}\sin\left[\frac{\pi}{2L}(2n+1)x\right]dx\ . \qquad (23)$$

Proceeding with the integration we obtain

$$\tilde{\theta}(t) = \frac{4}{\pi(\beta-\alpha)}\sum_{n=0}^{\infty}\frac{2Z_n}{(2n+1)\pi}\left[\cos\frac{\alpha\pi}{2}(2n+1)\right.$$

$$\left. - \cos\frac{\beta\pi}{2}(2n+1)\right]\ . \qquad (24)$$

Substituting Equation 23 into Equation 24 the final result becomes

$$\tilde{\theta}(t) = \frac{\tilde{N}-N_R}{N_o-N_R} = \frac{8}{\pi^2(\beta-\alpha)} \sum_{n=0}^{\infty} \frac{1}{(2n+1)^2} \exp\left[\frac{-4}{\pi^2}(2n+1)^2 \frac{Dt}{L^2}\right] \left[\cos\frac{\alpha\pi}{2}(2n+1) - \cos\frac{\beta\pi}{2}(2n+1)\right] . \quad (13)$$

APPENDIX B

The following pages include plots of the average diffusion coefficient from each capillary section versus the average of the initial capillary and reservoir compositions. The slope and intercept values are shown in Table 5.

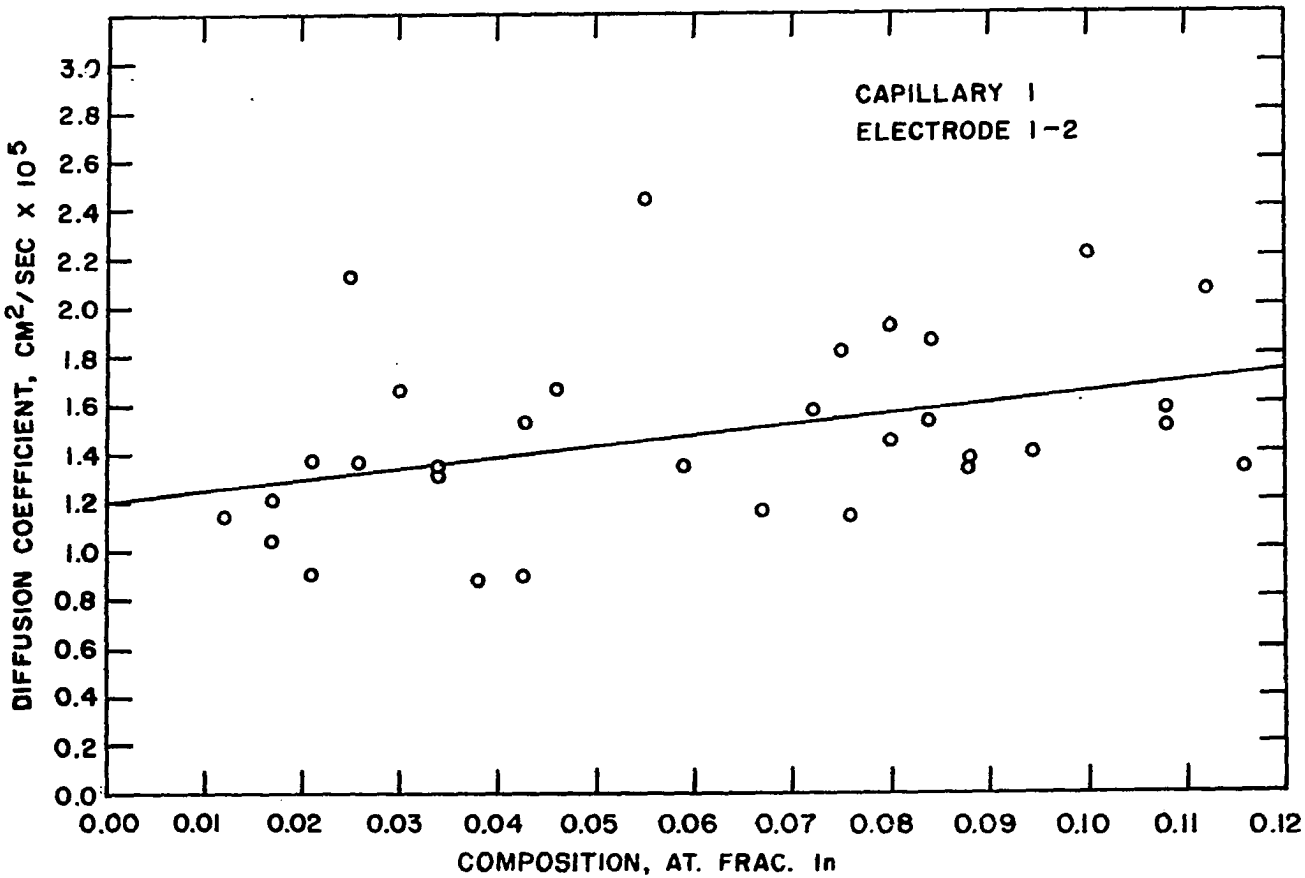

Figure 9. Diffusivity dependence on composition for Capillary 1, Section 1

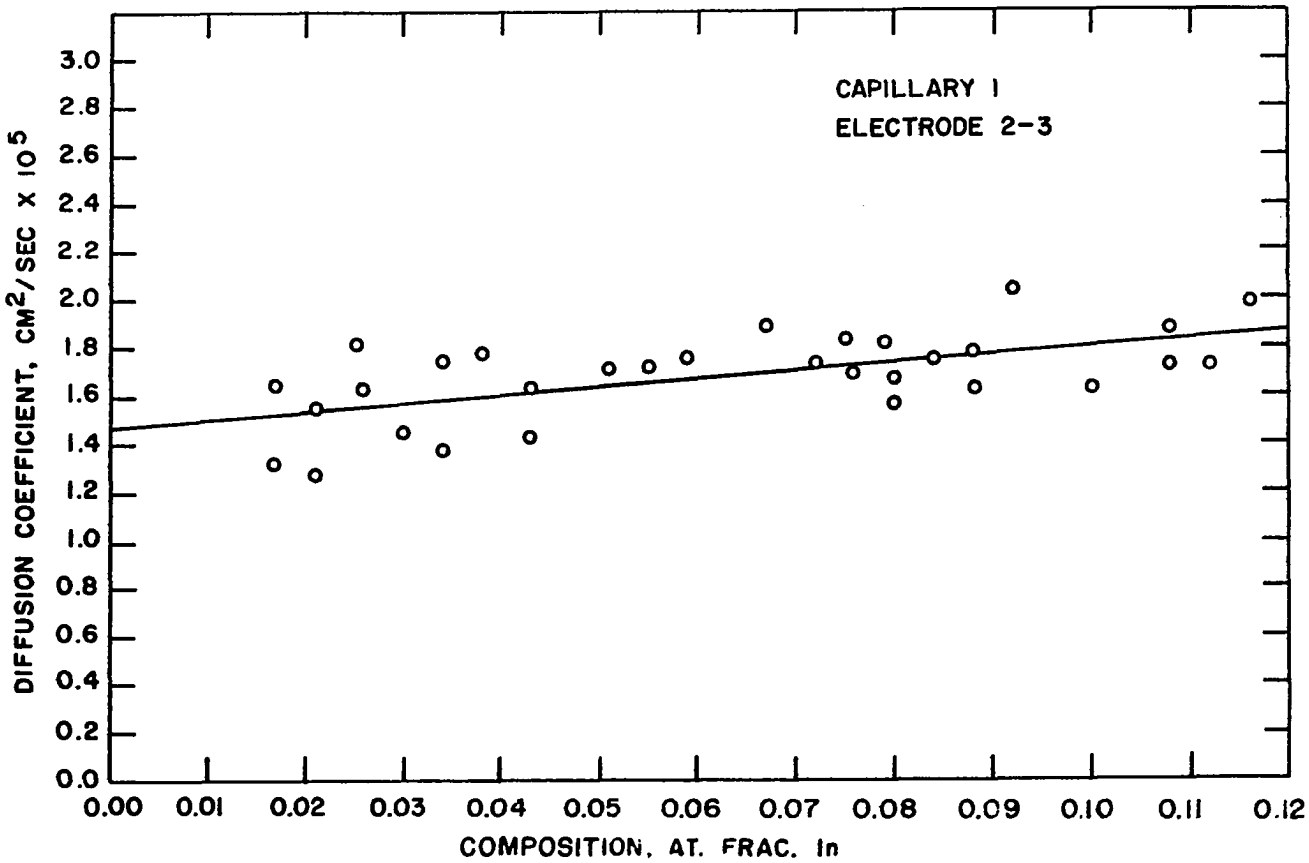

Figure 10. Diffusivity dependence on composition for Capillary 1, Section 2

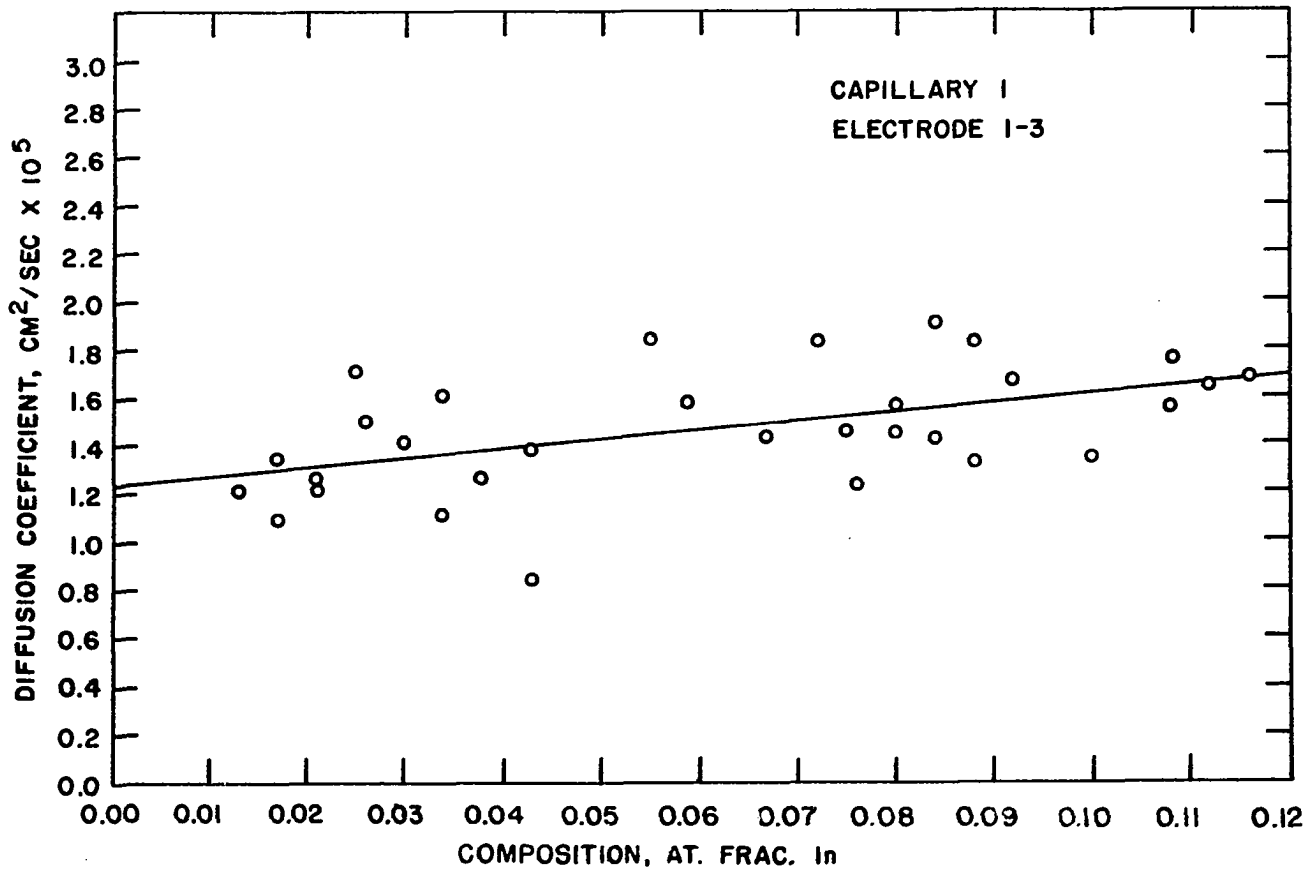

Figure 11. Diffusivity dependence on composition for Capillary 1, Section 3

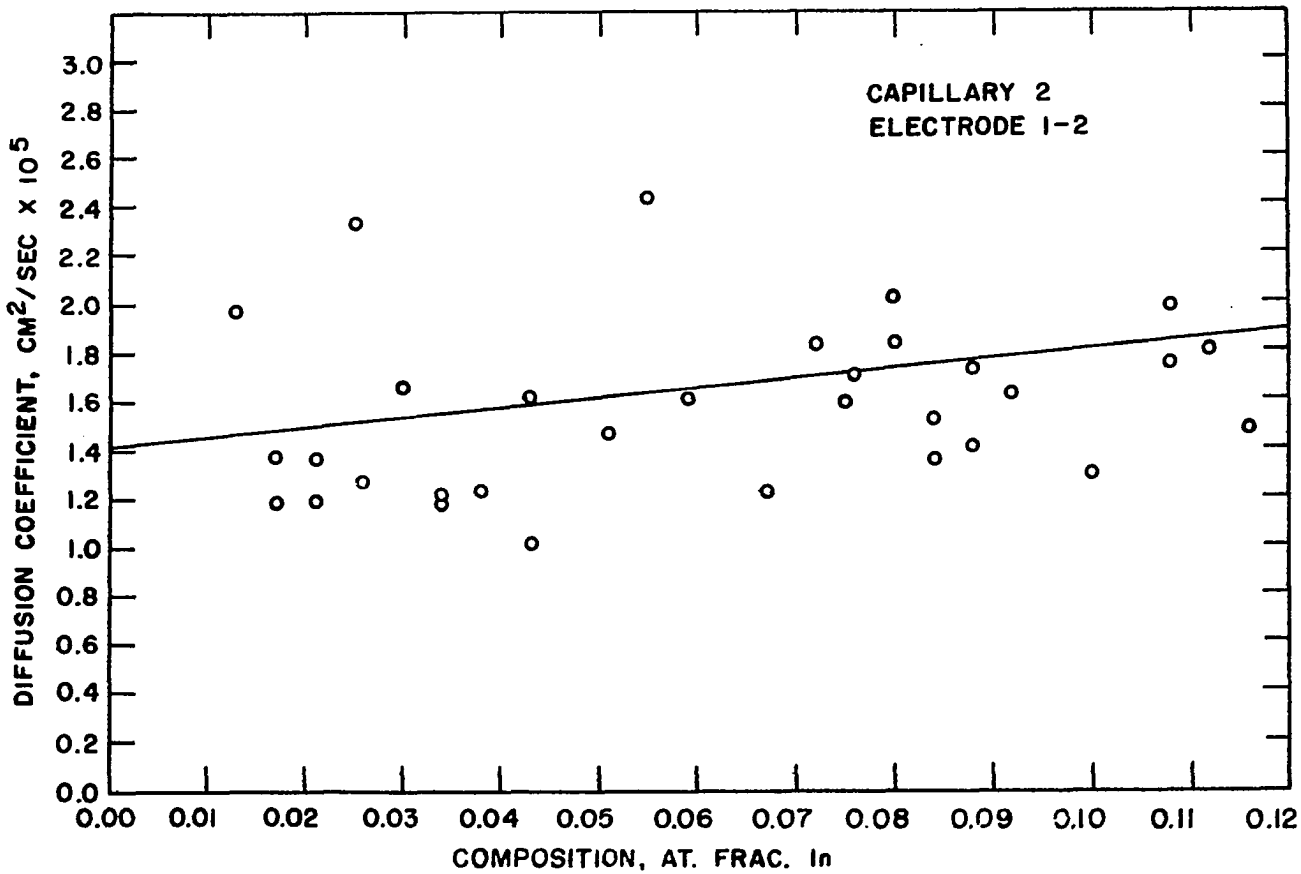

Figure 12. Diffusivity dependence on composition for Capillary 2, Section 1

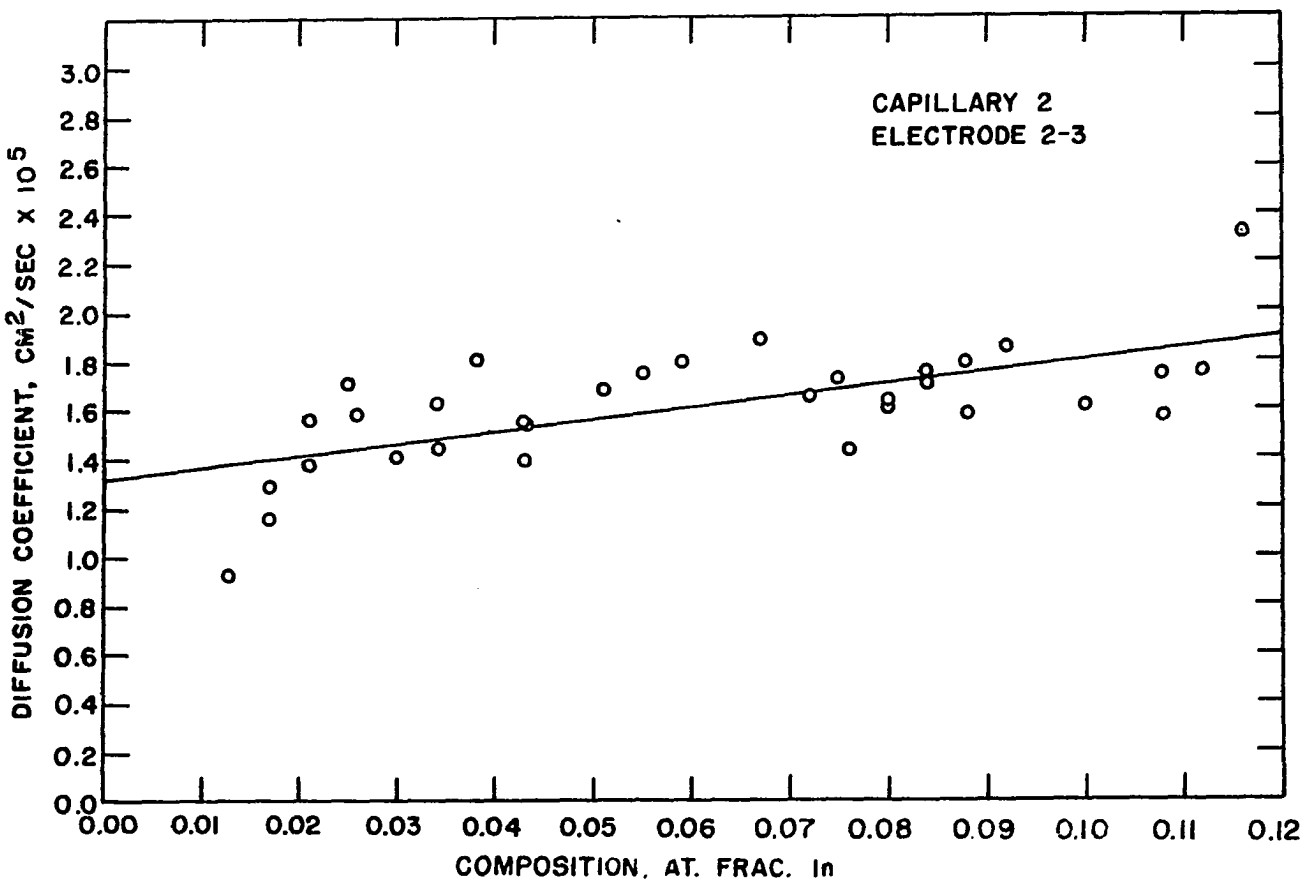

Figure 13. Diffusivity dependence on composition for Capillary 2, Section 2

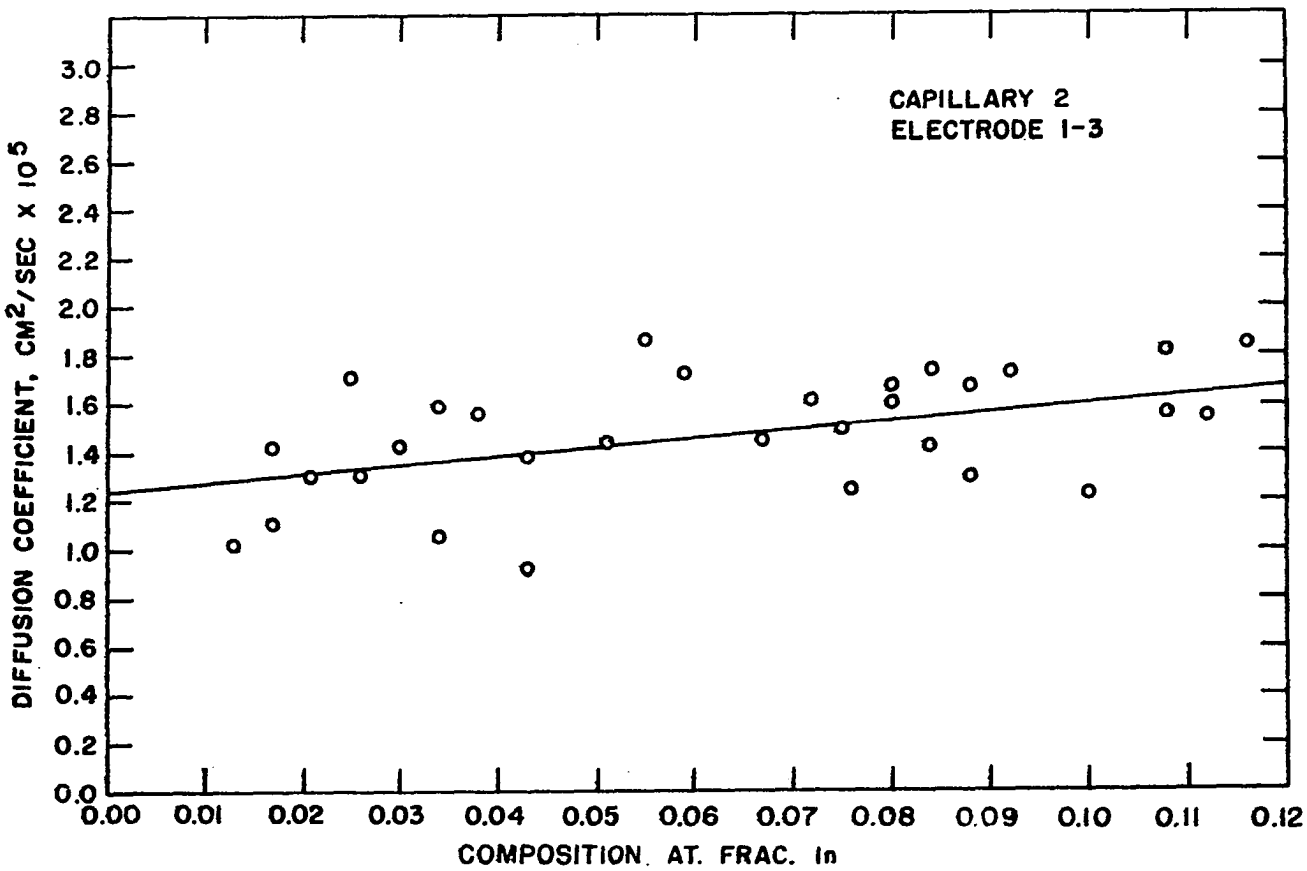

Figure 14. Diffusivity dependence on composition for Capillary 2, Section 3

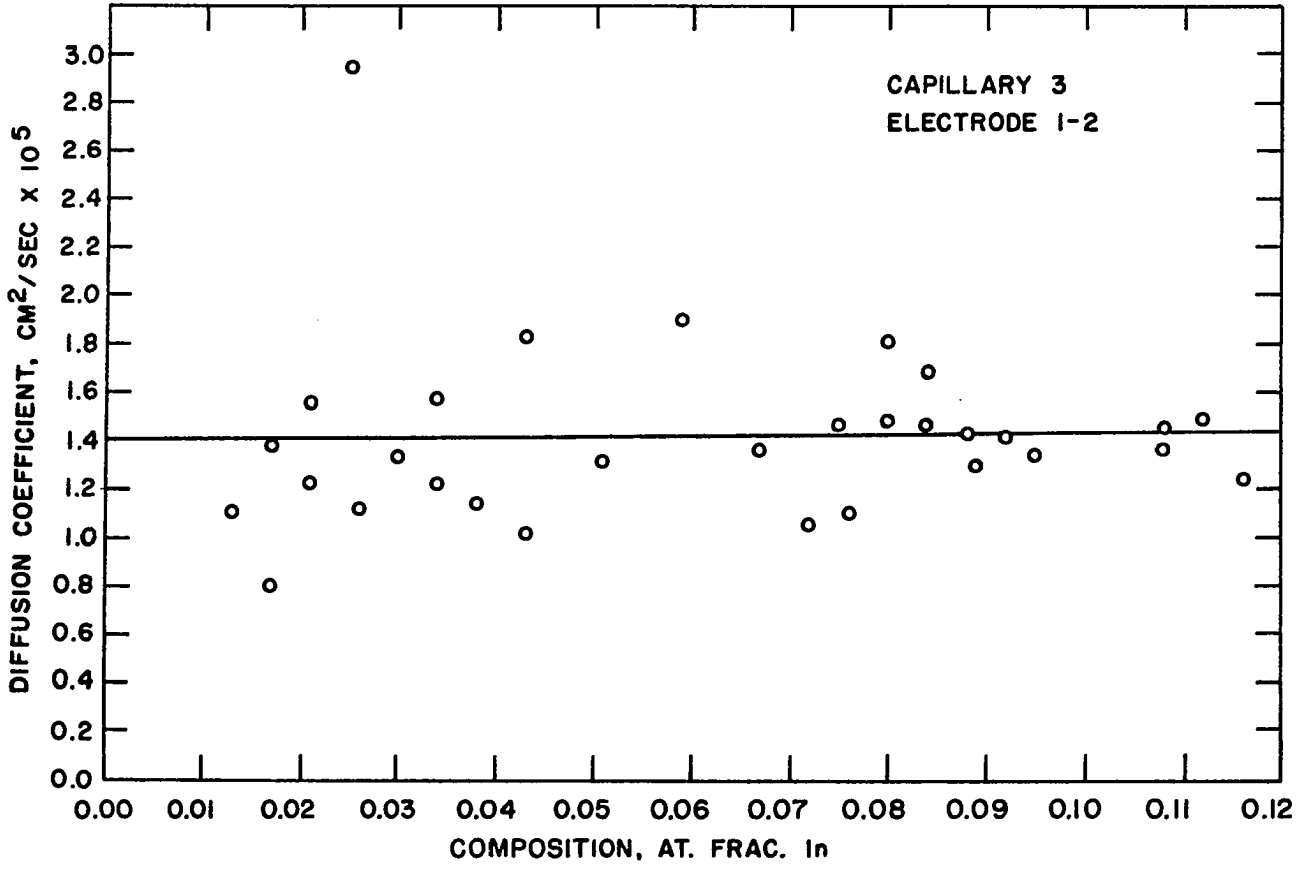

Figure 15. Diffusivity dependence on composition for Capillary 3, Section 1

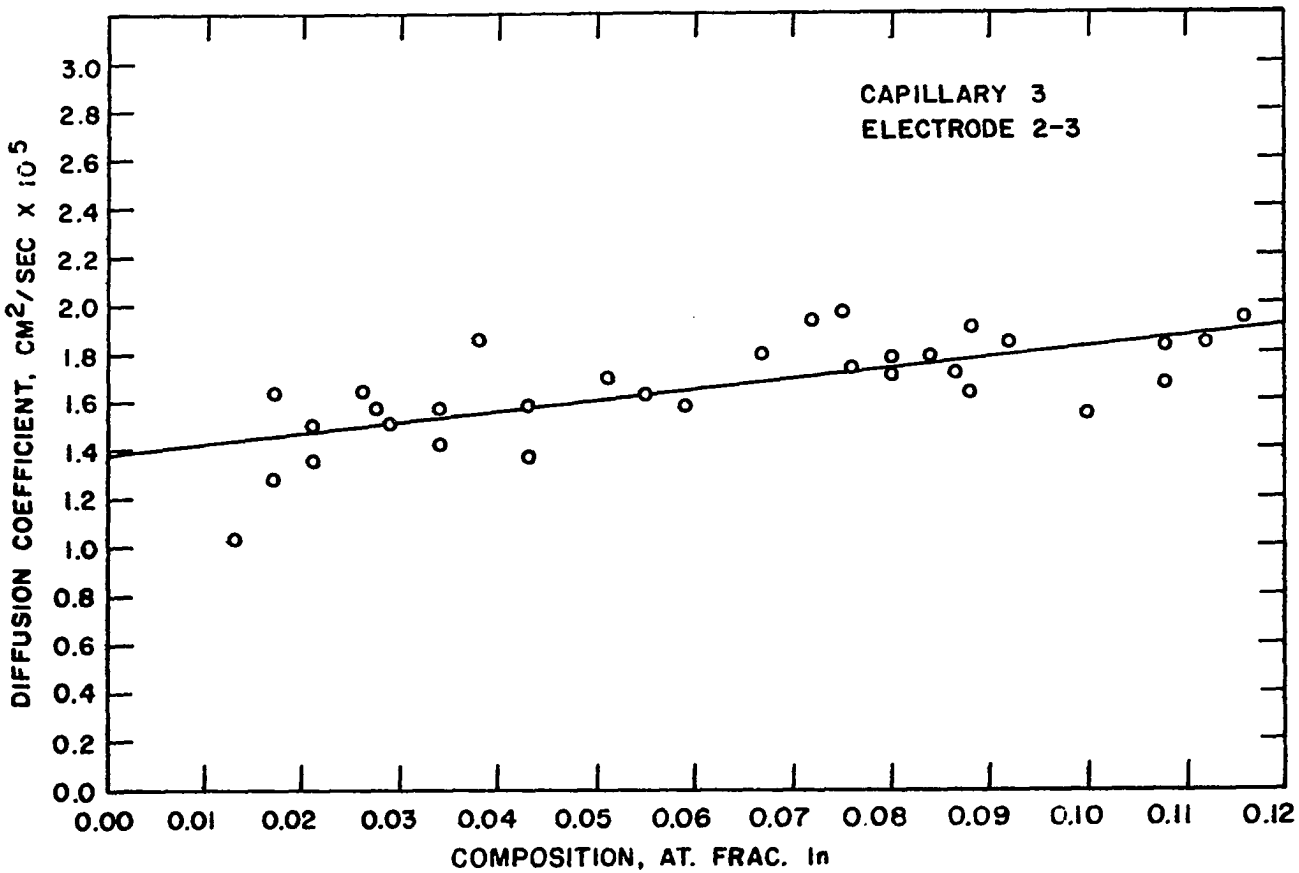

Figure 16. Diffusivity dependence on composition for Capillary 3, Section 2

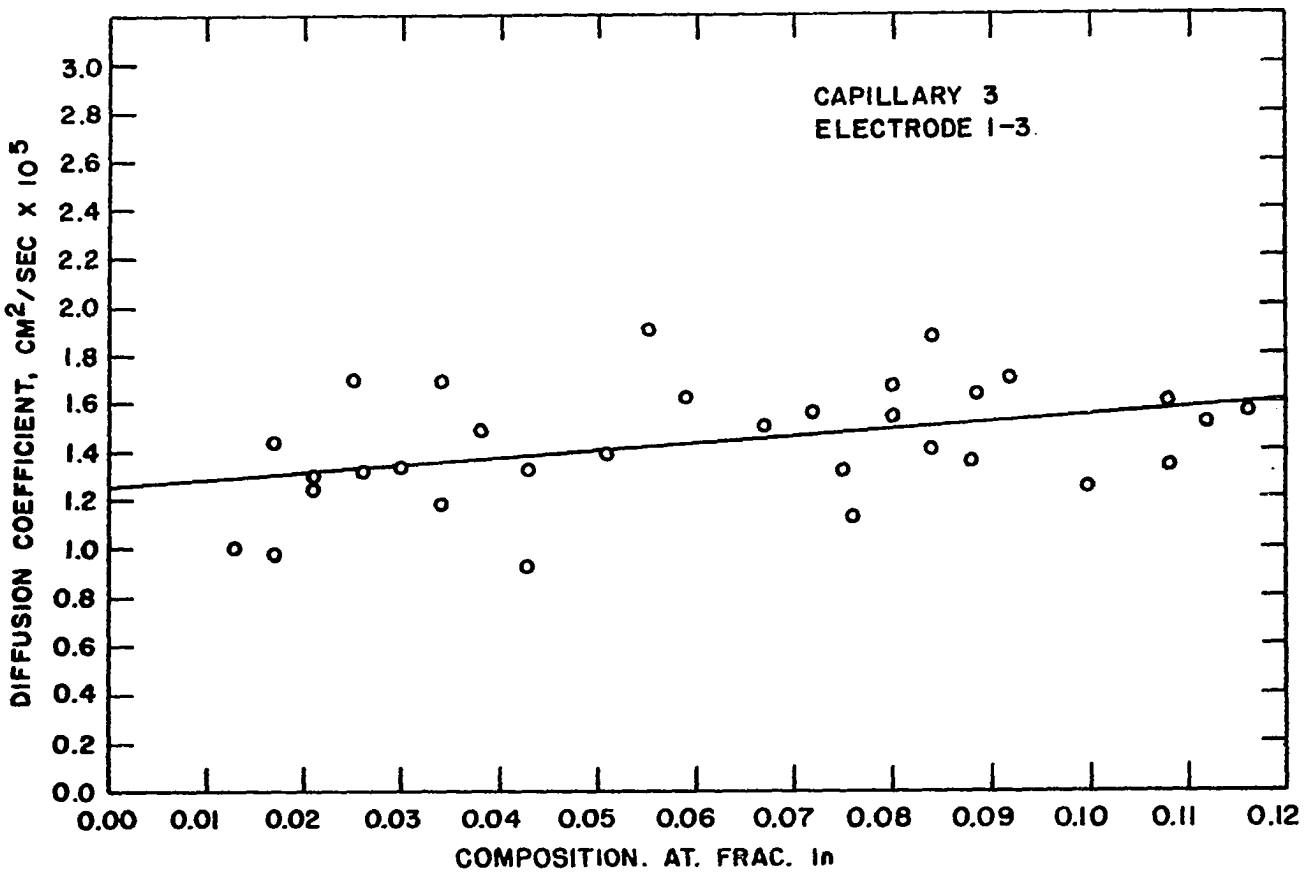

Figure 17. Diffusivity dependence on composition for Capillary 3, Section 3

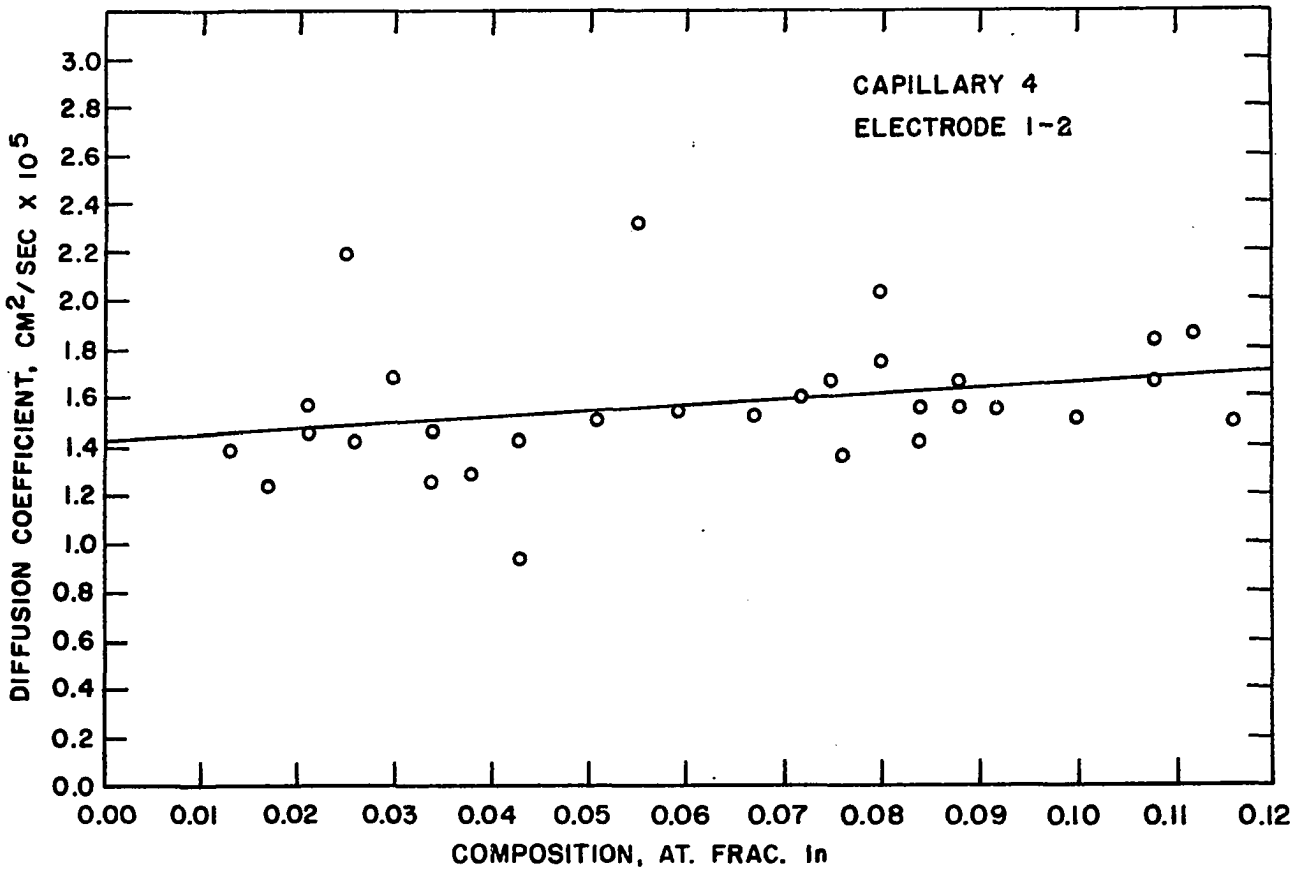

Figure 18. Diffusivity dependence on composition for Capillary 4, Section 1

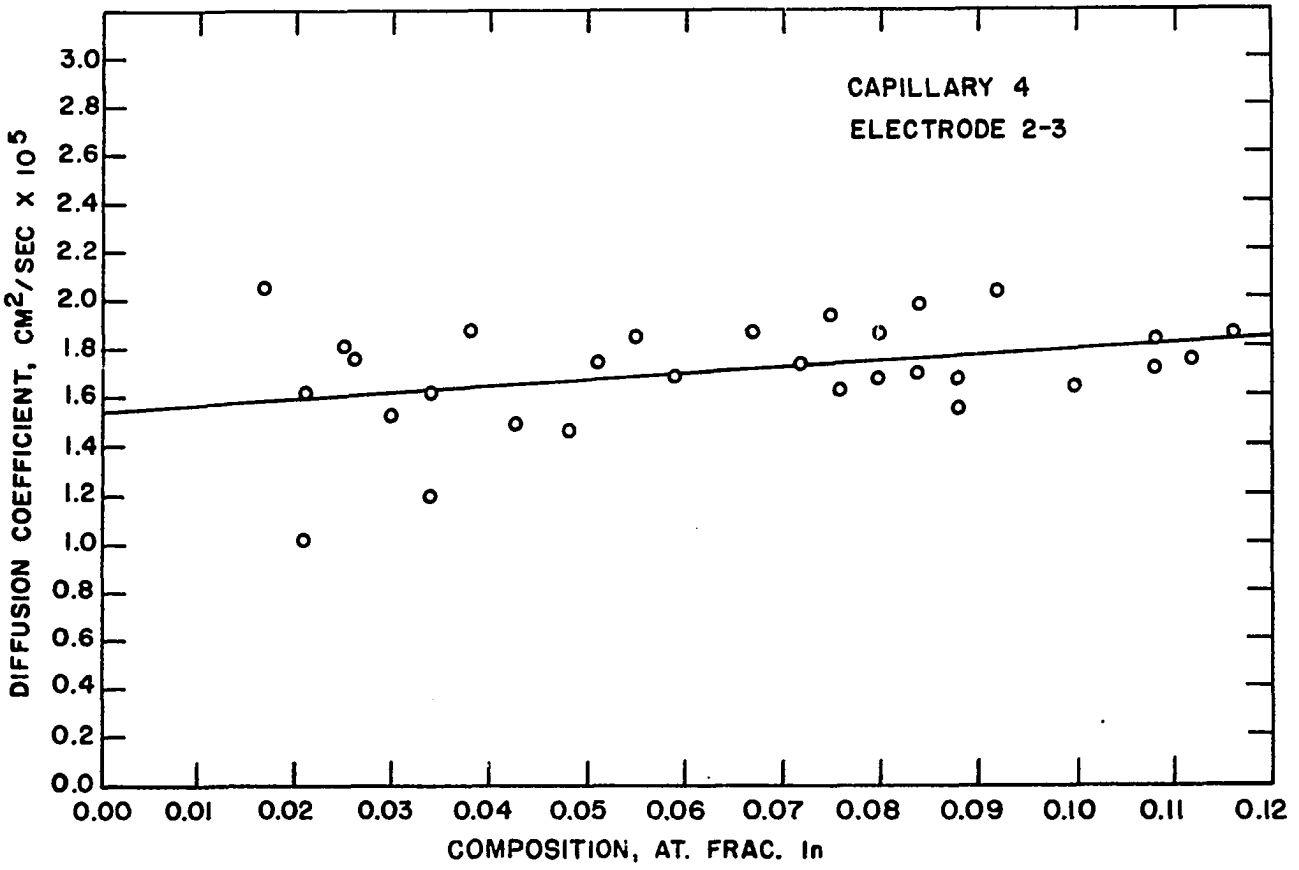

Figure 19. Diffusivity dependence on composition for Capillary 4, Section 2

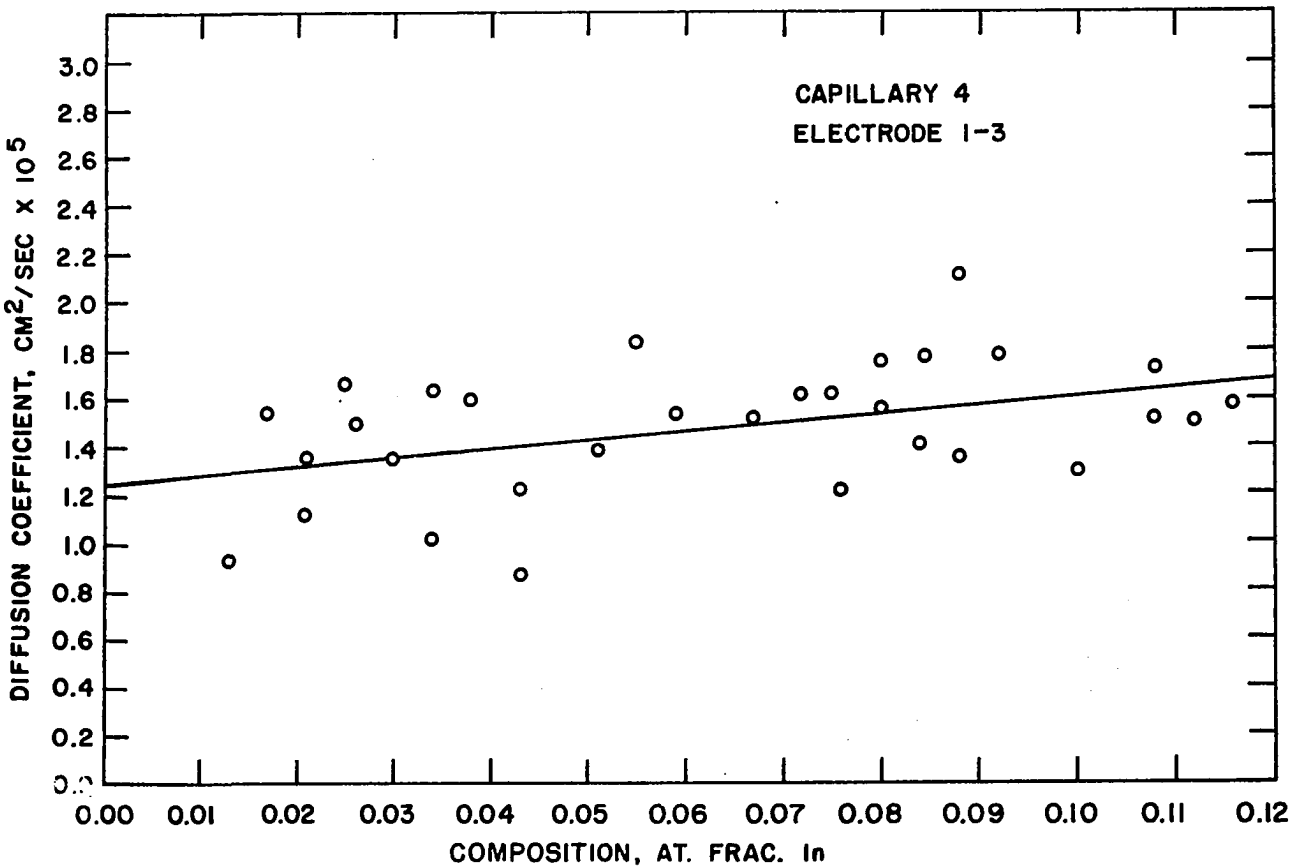

Figure 20. Diffusivity dependence on composition for Capillary 4, Section 3

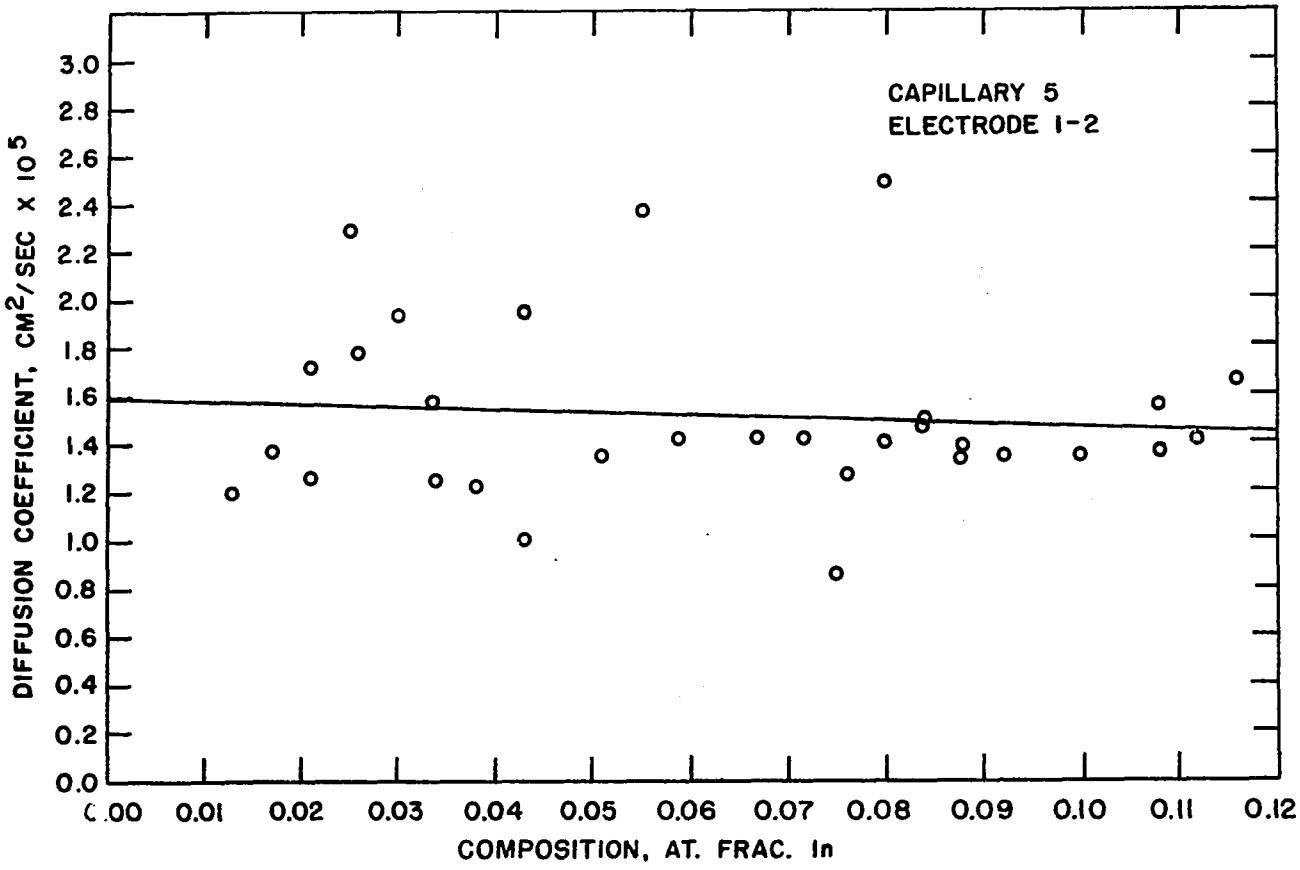

Figure 21. Diffusivity dependence on composition for Capillary 5, Section 1

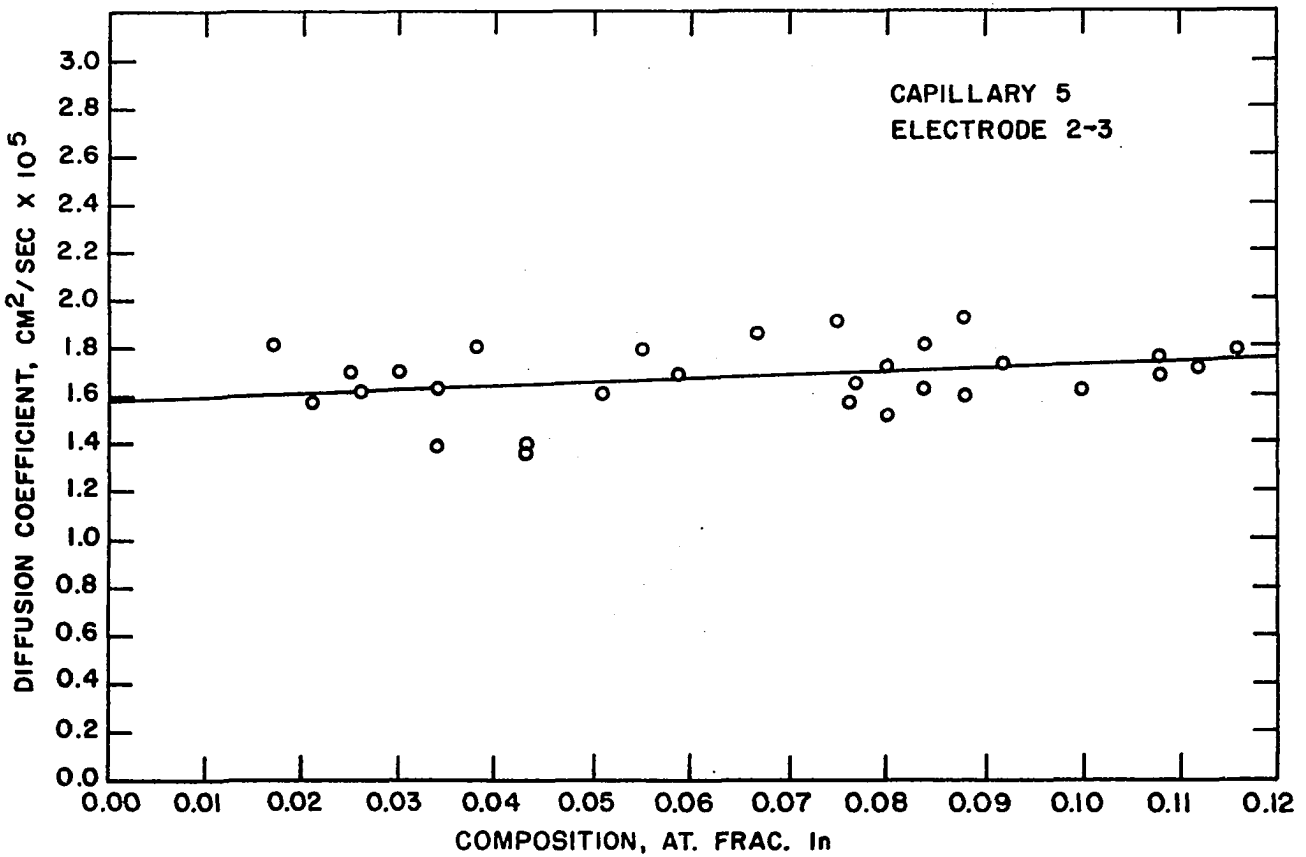

Figure 22. Diffusivity dependence on composition for Capillary 5, Section 2

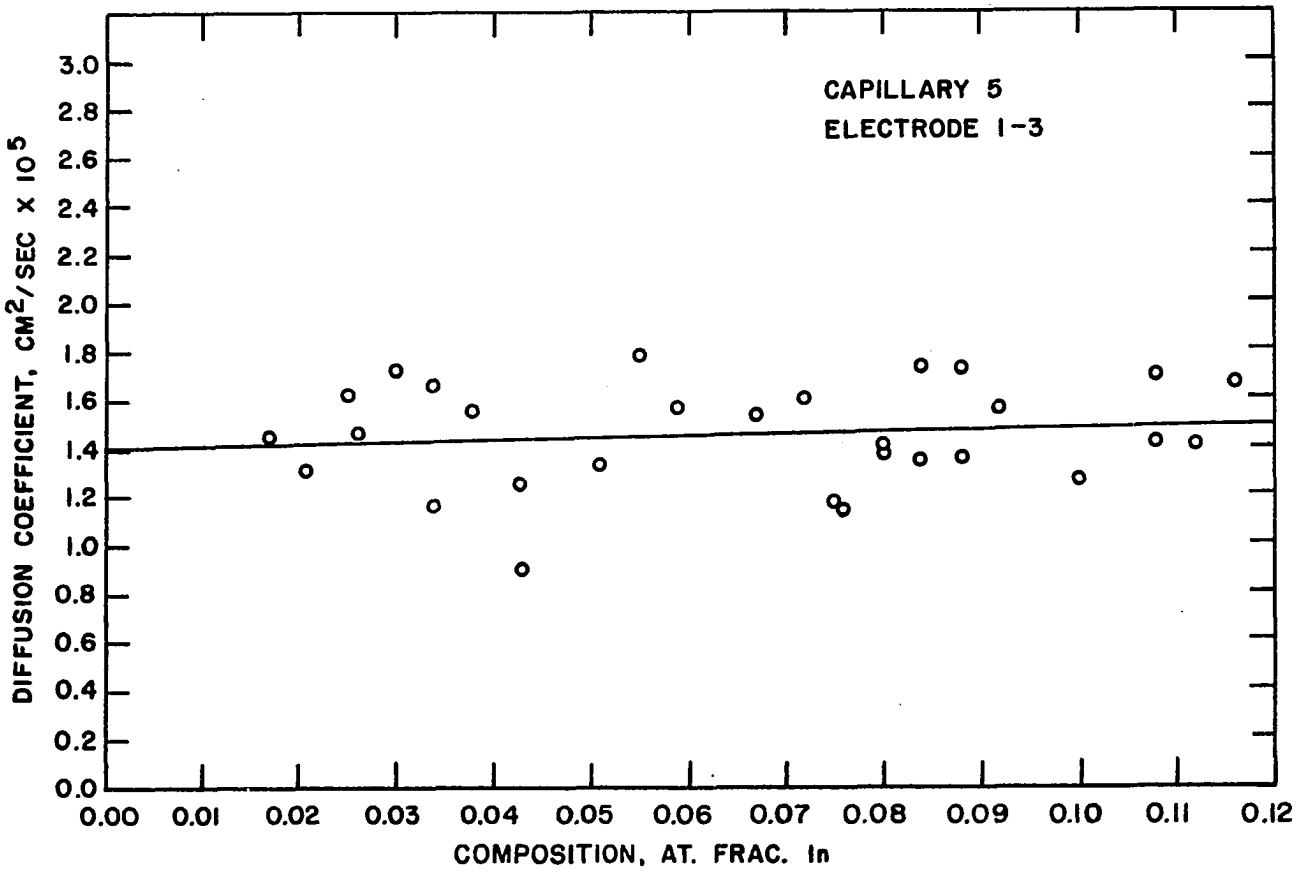

Figure 23. Diffusivity dependence on composition for Capillary 5, Section 3

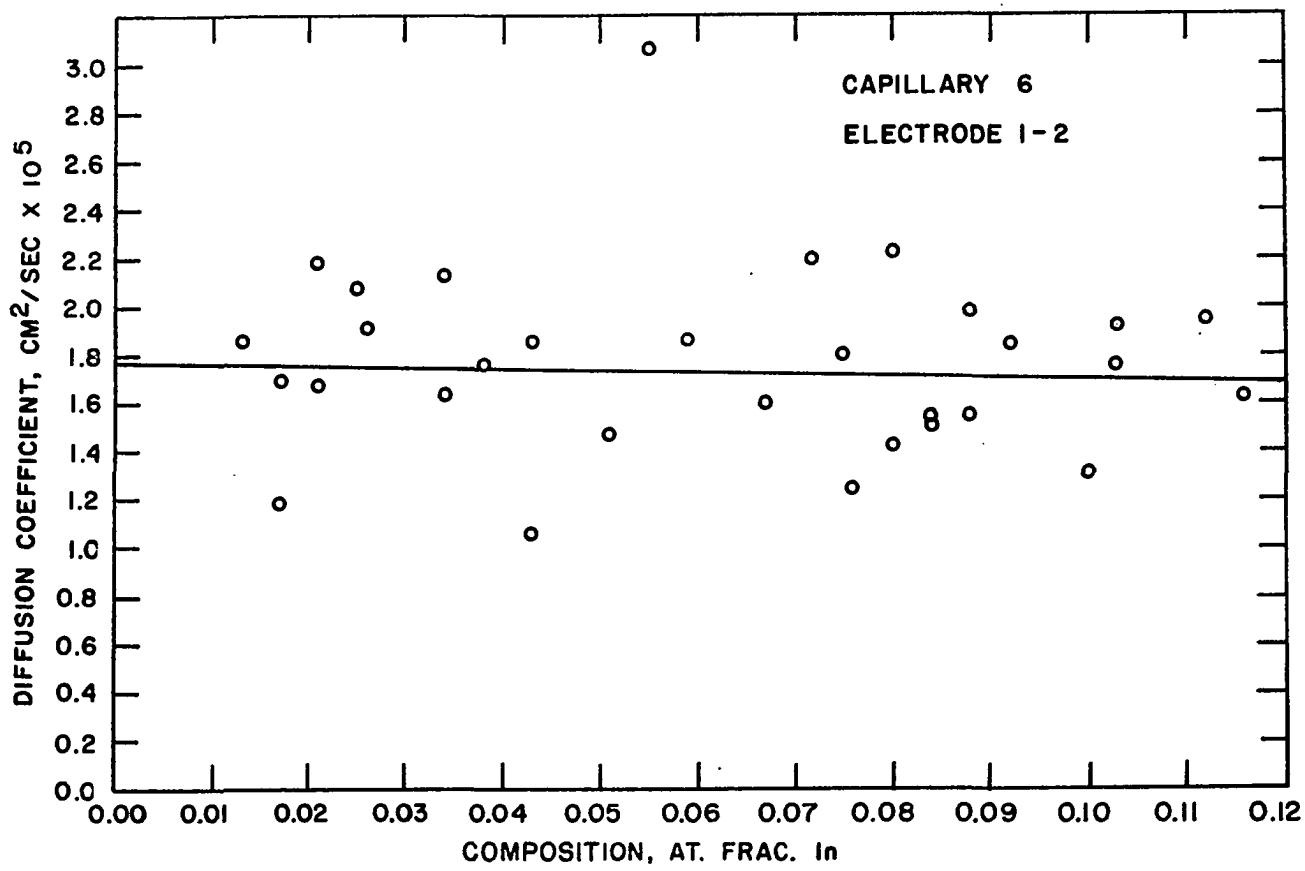

Figure 24. Diffusivity dependence on composition for Capillary 6, Section 1

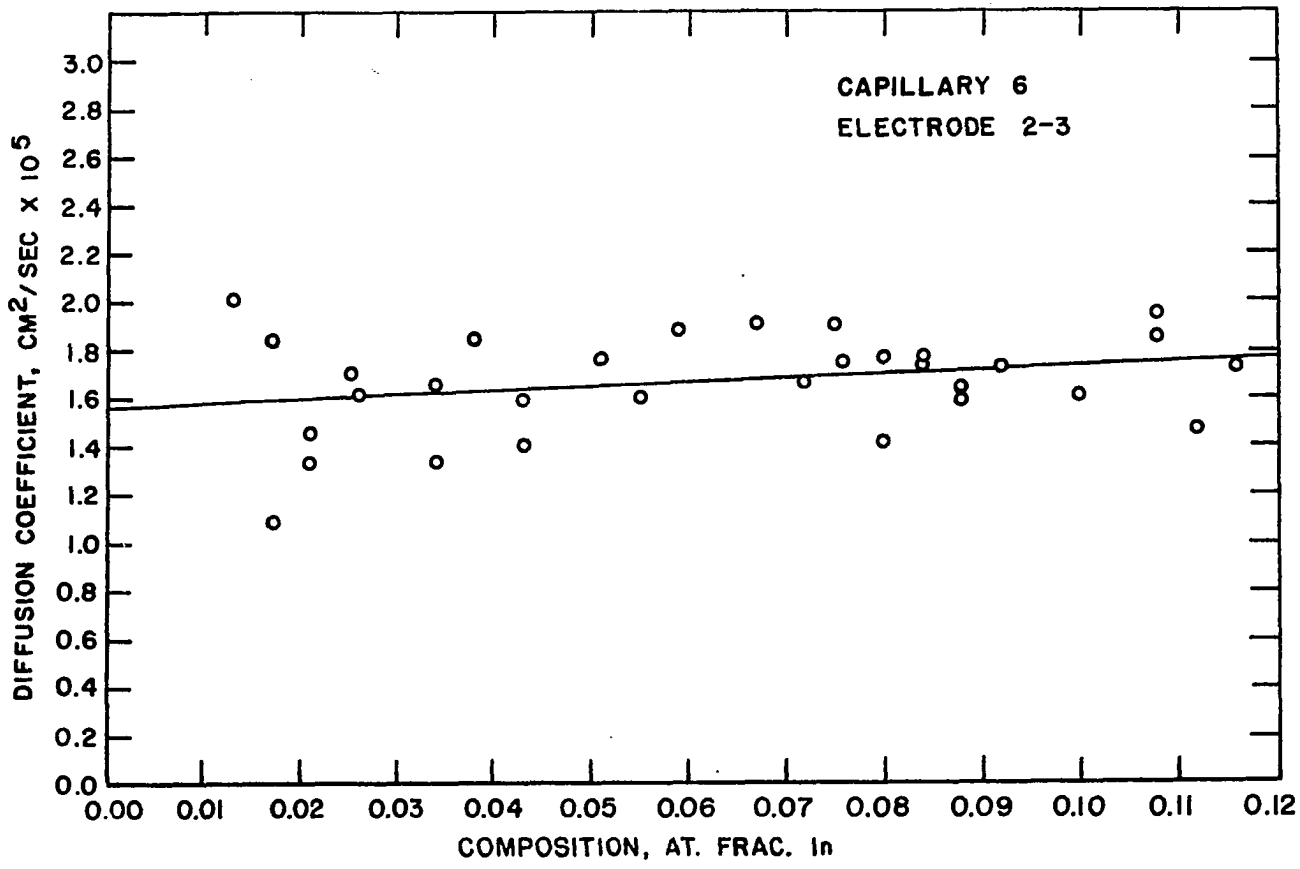

Figure 25. Diffusivity dependence on composition for Capillary 6, Section 2

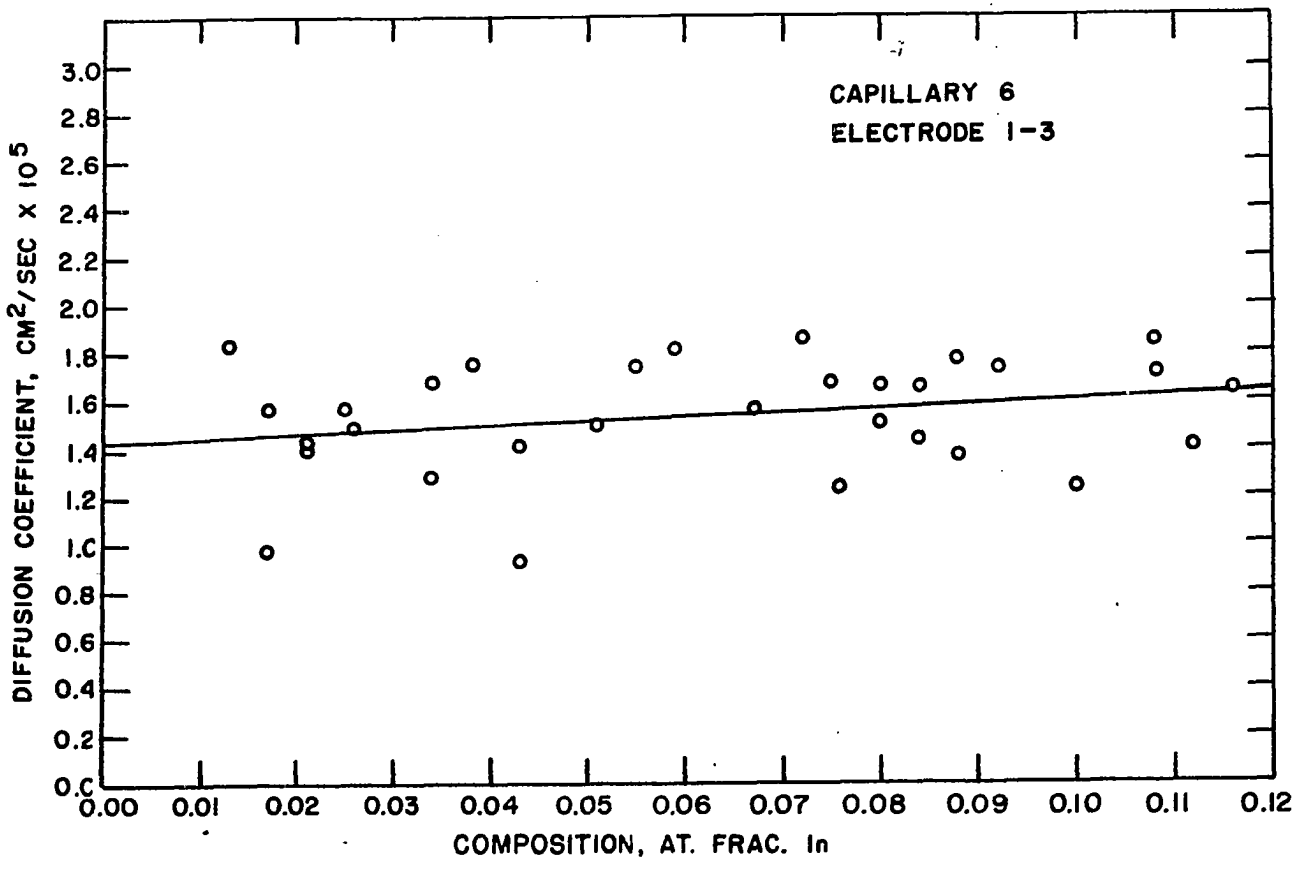

Figure 26. Diffusivity dependence on composition for Capillary 6, Section 3